

5

Title: T cell circuits that sense antigen density with an ultrasensitive threshold

10 **Authors:** Rogelio A. Hernandez-Lopez^{1,3}, Wei Yu¹, Katelyn A. Cabral^{2,3,4†}, Olivia A. Creasey^{2,3,4†}, Maria del Pilar Lopez Pazmino^{1,3}, Yurie Tonai¹, Arsenia De Guzman¹, Anna Mäkelä⁵, Kalle Saksela⁵, Zev J. Gartner^{2,3}, Wendell A. Lim^{1,3*}.

15

Affiliations:

20 ¹ Cell Design Institute, Department of Cellular and Molecular Pharmacology, University of California, San Francisco, CA, USA

² Department of Pharmaceutical Chemistry, Chan Zuckerberg BioHub, University of California San Francisco, San Francisco, CA, USA

25 ³ Center for Cellular Construction, University of California San Francisco, San Francisco, CA, USA

⁴ Graduate Program in Bioengineering, University of California Berkeley and University of California San Francisco

30 ⁵ Department of Virology, Haartman Institute, University of Helsinki, Finland.

†These authors contributed equally to this work

*Correspondence to: wendell.lim@ucsf.edu

35

Abstract:

5

Overexpressed tumor associated antigens (e.g. HER2 and epidermal growth factor receptor) are attractive targets for therapeutic T cells, but toxic “off-tumor” cross-reaction with normal tissues expressing low levels of target antigen can occur with Chimeric Antigen Receptor (CAR) T cells. Inspired by natural ultrasensitive response circuits, we engineered a two-step positive feedback circuit that allows T cells to discriminate targets based on a sigmoidal antigen density threshold. In this circuit, a low affinity synthetic Notch receptor for HER2 controls the expression of a high affinity CAR for HER2. Increasing HER2 density thus has cooperative effects on T cells -- it both increases CAR expression and activation -- leading to a sigmoidal response. T cells with this circuit show sharp discrimination between target cells expressing normal amounts of HER2 and cancer cells expressing 100-fold more HER2, both *in vitro* and *in vivo*.

10

15

One Sentence Summary:

20

Engineered T cells with a two-step positive feedback circuit are capable of killing target cancer cells with an ultrasensitive antigen density threshold.

25

MAIN TEXT

The specificity with which chimeric antigen receptor (CAR) T cells can recognize and kill tumor cells and discriminate against normal cells remains limited (1-3). A major challenge is finding surface proteins that are absolutely tumor specific (4). CAR T cells are effective in treating hematologic cancers (5-7), but they indiscriminately kill both cancerous and normal B cells because they target the lineage specific protein, CD19. Loss of B cells is tolerable, but killing of normal tissue when treating solid cancers with CAR T cells remains a major challenge that can lead to toxicity, and in some cases has proven lethal (8, 9, 10). Antigen receptors such as HER2 and epidermal growth factor (EGFR) are overexpressed in cancers, but they are also expressed at lower densities in normal epithelial tissues (11, 12). Thus, anti-HER2 CAR T cells have shown, in some cases, toxic cross-reaction with normal organs (8). Such on-target, off-tumor toxicity has been observed for CARs directed at several other overexpressed tumor-associated antigens (13, 14). While some toxicity cases can be managed clinically (9), ideally, engineered T cells should reliably discriminate cancer cells from normal cells based on antigen density (**Fig. 1A** top).

To widen their therapeutic window, engineered T cells must sense target antigen density with a sigmoidal response and a sharper killing threshold (**Fig. 1A** - bottom). Dose-response behaviors where small changes in input can generate large, non-linear changes in output activity, are referred to as “ultrasensitive” responses (15, 16).

Ultrasensitive behavior is observed in many critical regulatory systems, and can be achieved through various mechanisms, ranging from allosteric molecules (e.g. hemoglobin) to more complex regulatory cascades or circuits (17-19). Ultrasensitive circuits shift linear responses towards switch-like “all-or-none” responses in many biological systems (15, 18, 20). In T cells, for example, binding of the cytokine IL-2 to basally expressed low affinity receptors results in induced expression of the high affinity alpha subunit of the IL-2 receptor (CD25) (21). Thus, IL-2 acts on T cells in two ways – it both directly activates the cells while also making the cells more sensitive to IL-2 – thereby resulting in a form of positive feedback and cooperativity.

We used a modular approach to engineer ultrasensitive T cells (22-24). Our strategy was to first recognize the cognate antigen with a low-affinity synthetic notch (synNotch) receptor, which would, in turn, induce expression of a high-affinity CAR for the same antigen (**Fig. 1B**) (SynNotch receptors activate transcription of a genetically encoded payload when they engage input ligand (23-25)). In this circuit design, the low-affinity synNotch receptor acts as a filter,

constraining transcription induction to only occur when the T cell encounters target cells with high antigen expression. Once past this initial filter, the induced high-affinity CAR permits strong T cell killing and proliferation. Together, the circuit could yield an all-or-none, ultrasensitive response.

To evaluate T cell circuits engineered to achieve density-dependent recognition of the HER2 antigen, we constructed a series of stable human leukemia (K562) tumor cell lines that differ only in their amount of HER2 expression over a 100-fold range (**Fig. 1C**). The HER2 densities correspond to those of several cancer cell lines (**Fig. S1A**). A clinically relevant goal is to be able to reliably discriminate between cells expressing $>10^{6.5}$ (HER2 pathology score of 3+, as defined by ASCO-CAP scoring guidelines) vs $10^{4.5}$ molecules per cell (HER2 score of 0 or 1+, termed HER2 negative), as these are the expression amounts found in several HER2 amplified cancers and several normal HER2 expressing human tissue samples (26), respectively. To build the synNotch receptors and CARs, we made a series of anti-HER2 single chain antibodies (scFv) with affinities that span a 100-fold range (dissociation constants between 2.0 nM and 200 nM; **Fig. 1D**, **Fig. S2**).

We constructed and tested several versions of the anti-HER2 synNotch → anti-HER2 CAR circuit in human primary CD8+ T cells *in vitro* (**Fig. S3A**). To assay density sensing behavior, we measured target cell killing by quantitative flow cytometry. Several circuit T cells showed antigen density ultrasensitivity (Hill coefficients (n_H) of 1.7 - 4.4) (**Fig. 2A** bottom). In contrast, T cells with constitutive expression of either high- or low-affinity CAR showed little density discrimination (**Fig. 2A** top). In circuit T cells in which a low-affinity synNotch receptor (scFv K_d 210 nM) was used to control expression of a high-affinity CAR receptor (scFv K_d 17.6 nM) (**Fig. 2A**, red line), their ultrasensitive threshold clearly discriminated between the target densities of $10^{4.5}$ and $10^{6.5}$ (**Fig. 2B**, $n_H = 4.4$, $\text{den}_{50} = 10^{5.5}$; see **Fig. S4B** for circuit activity in T cells from multiple donors).

The observed ultrasensitivity appears to originate from the designed transcriptional cascade. Steady state amounts of CAR expression (monitored by tagging CARs with a mCherry protein, **Fig. S3A**) depended strongly on target antigen density (**Fig. 2B** left, **Fig. S4C** red line). T cell proliferation, a critical component of an antitumor response, also showed an ultrasensitive dependence on target antigen density (**Fig. 2B** right, **Fig. S4C** green line).

The response of the T cell circuit could be tuned by altering the receptor affinities within the circuit. For example, lowering the CAR affinity (scFv K_d 210 nM) (while maintaining a low-affinity synNotch) increased the density threshold (**Fig. S4D**) ($\text{dens}_{50} = 10^{6.0}$), but also reduced maximal killing activity and lowered overall ultrasensitivity ($n_H = 1.7$). Ultrasensitivity began to break down if we use a medium-affinity synNotch (scFv K_d 46.5 nM) receptor as the circuit filter (**Fig. S4D** brown line). Thus, robust ultrasensitive response is generated by linking low- and high-affinity recognition into a two-step cascade (**Fig. 2C**). Low-affinity synNotch receptors that encounter low densities of HER2 antigen produce low amounts of CAR expressed at the T cell surface (**Fig. 2C** left). In contrast, when low-affinity synNotch receptors encounter high HER2 densities (**Fig. 2C** right) they express higher steady-state amounts of CAR. Thus, high target antigen density both increases CAR expression level and activates T cell proliferation and killing, leading to a non-linear all-or-none response (**Fig. 2C**).

In contrast, we found that constitutively expressed CARs, even with reduced CAR expression or affinity (**Fig. S3B**), triggered T cell killing of low density antigen cells (**Fig. S5A,B**). CAR and synNotch receptors showed different sensitivities, even when using the same antigen binding domain. CARs are more sensitive, triggering killing activity with relatively low antigen density (**Fig. 2A**, **Fig. S5**), while synNotch mediated gene expression requires higher antigen densities. Thus, the low affinity synNotch receptor does not induce a sufficient amount of CAR expression to trigger a killing response with low density targets and only initiates strong killing with high density targets (**Fig. 2A** bottom, **Fig. 2B**, **Fig. S4C**).

We further tested the synNotch_{low affinity} → CAR_{high affinity} (scFv K_d 210 nM synNotch, 17.6 nM CAR) HER2 antigen density sensing circuit against a number of different human cancer cell lines with low and high HER2 expression (**Fig. 3A,B; Fig. S6**). In *in vitro* killing assays, engineered T cells were mixed with target cancer cells expressing either low density HER2 (human prostate adenocarcinoma, PC3, $10^{4.8}$ HER2 molec./cell, HER2 score 1+) or high density HER2 (human ovary adenocarcinoma, SKOV3, $10^{7.0}$ HER2 molec./cell, HER2 score 3+). With the low HER2 density cells, neither the untransduced T cells nor the synNotch_{low affinity} → CAR_{high affinity} circuit T cells showed cytotoxicity over 72 hours (**Fig. 3B, Movie S2**). For the high HER2 density cells, the synNotch_{low affinity} → CAR_{high affinity} circuit T cells effectively killed the high HER2 cells (**Movie S2**). Notably, however, we observed delayed activation onset and a lag in the time required for complete killing compared to T cells with constitutive CAR

expression (72 hrs. vs 24 hrs.) (**Movie S1**). This delay is consistent with a model in which CAR expression mediated by synNotch recognition requires additional time to accumulate sufficient CAR for effective killing (**Fig. 3B**). Similar discriminatory behavior was observed against other human cancer lines of varying HER2 densities (**Fig. S6A,B**). In contrast, the constitutive CAR T cells (both high and low affinity CAR) rapidly eliminated both the low and high HER2 target cells in this assay (**Fig. S5D; S6A,B** and **Movie S1**). In the circuit T cells, CAR expression and T cell proliferation also showed a clear dependence on input HER2 antigen density (**Fig. S6C** top row). In summary, the $\text{synNotch}_{\text{low affinity}} \rightarrow \text{CAR}_{\text{high affinity}}$ T cells significantly improve discrimination between multiple high and low density cancer cells, but the timing of circuit activation results in delayed onset of tumor killing.

To evaluate how these ultrasensitive density sensing T cells behave in a more complex multicellular context, we used a 3D target spheroid culture model (27, 28). We engineered a human breast epithelial MCF10A line, that normally expresses low amounts of HER2 ($10^{4.7}$ HER2 molec./cell, HER2 score 0), to express high HER2 (equivalent to HER2 score 3+) (**Fig. 3C**). We assembled 3D spheroids (29) using either low or high HER2 MCF10A cells and embedded them in Matrigel with engineered T cells. Using 3D confocal microscopy and a caspase activity dye, we quantified the caspase fluorescence per spheroid over 3 days as an assay for target cell killing (**Fig. 3C**). The two-step circuit $\text{synNotch}_{\text{low affinity}} \rightarrow \text{CAR}_{\text{high affinity}}$ (scFv K_d 210 nM synNotch, 17.6 nM CAR) T cells effectively invaded, killed, and disassembled the high HER2 density spheroids, but discriminated against the low HER2 spheroids (**Fig. 3D, E right**). In contrast, a low-affinity anti-HER2 CAR killed and disassembled the low and high HER2 density spheroids indiscriminately (**Fig. 3D, E middle**).

We also used this spheroid assay to evaluate the degree of spatial discrimination. If a circuit T cell was activated by a high density spheroid, could it then migrate to a low density spheroid and kill those cells? We mixed a low number of high HER2 spheroids with an excess of low HER2 spheroids and T cells, all embedded in Matrigel. T cells were observed to migrate freely among the spheroids (**Fig. 3F; Fig. S7B,C**). We then measured the caspase signal within the low HER2 spheroids as a function of radial distance from the closest high HER2 spheroid (**Fig. 3F**). We found a very sharp decay of killing activity as a function of distance from the high HER2 spheroid and estimated a radius of off-target killing to be $<100 \mu\text{m}$ (**Fig. 3G**). The circuit T cells only infiltrated, expanded and launched a killing response in high antigen density spheroids

(**Fig. S7B,C**). Many aspects of T cell activation, including increased adhesion and production of local cytokine gradients, may contribute to this high level of spatial discrimination.

Finally, we evaluated density discrimination of synNotch_{low affinity} → CAR_{high affinity} (scFv Kd 210 nM synNotch, 17.6 nM CAR) circuit T cells in multiple mouse tumor models (**Fig. 4A**). We first

5 implanted immunocompromised NOD scid gamma (NSG) mice, with a high HER2 density K562 tumor on one side, and a low HER2 density K562 tumor on the opposite side. After establishing

the tumors, we injected the tail vein with a mix of equal numbers of CD4+ and CD8+ primary human T cells transduced with the synNotch_{low affinity} → CAR_{high affinity} circuit. The circuit T cells showed strong density discrimination (**Fig. 4B**, **Fig. S9A**) -- the high density tumors were

10 cleared rapidly, but the low density tumors grew at similar rates as observed with untransduced T cells. This tumor discrimination was also observed at a 5-fold higher effector to target ratio (**Fig. S12**).

The circuit T cells show significant expansion and induced CAR expression only within the high density tumors (**Fig. 4C,D**, **Fig. S11**). Consistent discrimination was observed with other pairs of human cancer cell lines expressing high (~10^{7.0} molec./cell) or low (~10⁵

15 molec./cell) amounts of HER2 (**Fig. 4E,F**, **Fig. S9B,C**). We performed control experiments with untransduced T cells (**Fig. S10**) or T cells constitutively expressing either a low- or a high-affinity anti-HER2 CAR (**Fig. S8**). The constitutive low- or high-affinity CAR T cells showed poor density discrimination, clearing both the low and high density tumors (**Fig. S8**).

This work demonstrates that a general design principle -- the use of a two-step regulatory circuit to generate an ultrasensitive dose-response behavior – can be used to engineer T cells that

20 discriminate between target cells with high and low antigen density expression. These two-step synNotch to CAR circuits function well both *in vitro* and *in vivo*, and the threshold can be tuned by altering the affinities of the synNotch and CAR receptors. This approach should enable

expansion of the repertoire of target antigens to include other examples that are overexpressed in 25 cancer cells compared to normal cells. Indeed, we were able to show that engineered T cells with a low affinity SynNotch receptor to high affinity CAR circuit, built from anti-EGFR binding domains (30, 31), resulted in ultrasensitive EGFR density sensing T cells (**Fig. S13**).

Effective deployment of therapeutic T cells to treat solid tumors will require overcoming several 30 other challenges including tumor heterogeneity, suppressive tumor microenvironments and improving trafficking of cells to the tumors. However, the ability to achieve ultrasensitive antigen density discrimination provides a critical tool for widening the therapeutic window of

engineered T cells against solid cancers, in which many tumor-associated antigens are overexpressed but not absolutely unique.

REFERENCES

1. W. A. Lim, C. H. June, The Principles of Engineering Immune Cells to Treat Cancer. *Cell* **168**, 724-740 (2017).
2. L. M. Whilding, J. Maher, CAR T-cell immunotherapy: The path from the by-road to the freeway? *Mol Oncol* **9**, 1994-2018 (2015).
3. J. N. Brudno, J. N. Kochenderfer, Chimeric antigen receptor T-cell therapies for lymphoma. *Nat Rev Clin Oncol* **15**, 31-46 (2018).
4. M. M. D'Aloia, I. G. Zizzari, B. Sacchetti, L. Pierelli, M. Alimandi, CAR-T cells: the long and winding road to solid tumors. *Cell Death Dis* **9**, 282 (2018).
5. S. L. Maude *et al.*, Tisagenlecleucel in Children and Young Adults with B-Cell Lymphoblastic Leukemia. *N Engl J Med* **378**, 439-448 (2018).
10. S. S. Neelapu *et al.*, Axicabtagene Ciloleucel CAR T-Cell Therapy in Refractory Large B-Cell Lymphoma. *N Engl J Med* **377**, 2531-2544 (2017).
15. S. J. Schuster *et al.*, Tisagenlecleucel in Adult Relapsed or Refractory Diffuse Large B-Cell Lymphoma. *N Engl J Med* **380**, 45-56 (2019).
20. R. A. Morgan *et al.*, Case report of a serious adverse event following the administration of T cells transduced with a chimeric antigen receptor recognizing ERBB2. *Mol Ther* **18**, 843-851 (2010).
25. C. H. Lamers *et al.*, Treatment of metastatic renal cell carcinoma with CAIX CAR-engineered T cells: clinical evaluation and management of on-target toxicity. *Mol Ther* **21**, 904-912 (2013).
30. F. C. Thistlethwaite *et al.*, The clinical efficacy of first-generation carcinoembryonic antigen (CEACAM5)-specific CAR T cells is limited by poor persistence and transient pre-conditioning-dependent respiratory toxicity. *Cancer Immunol Immunother* **66**, 1425-1436 (2017).
35. A. McCabe, M. Dolled-Filhart, R. L. Camp, D. L. Rimm, Automated quantitative analysis (AQUA) of *in situ* protein expression, antibody concentration, and prognosis. *J Natl Cancer Inst* **97**, 1808-1815 (2005).
40. W. Yasui *et al.*, Expression of epidermal growth factor receptor in human gastric and colonic carcinomas. *Cancer Res* **48**, 137-141 (1988).
12. M. R. Parkhurst *et al.*, T cells targeting carcinoembryonic antigen can mediate regression of metastatic colorectal cancer but induce severe transient colitis. *Mol Ther* **19**, 620-626 (2011).
13. Y. Guo *et al.*, Phase I Study of Chimeric Antigen Receptor-Modified T Cells in Patients with EGFR-Positive Advanced Biliary Tract Cancers. *Clin Cancer Res* **24**, 1277-1286 (2018).
14. Q. Zhang, S. Bhattacharya, M. E. Andersen, Ultrasensitive response motifs: basic amplifiers in molecular signalling networks. *Open Biol* **3**, 130031 (2013).
15. S. A. Frank, Input-output relations in biological systems: measurement, information and the Hill equation. *Biol Direct* **8**, 31 (2013).
16. S. Hooshangi, S. Thiberge, R. Weiss, Ultrasensitivity and noise propagation in a synthetic transcriptional cascade. *Proc Natl Acad Sci U S A* **102**, 3581-3586 (2005).

18. J. E. Ferrell, Jr., S. H. Ha, Ultrasensitivity part III: cascades, bistable switches, and oscillators. *Trends Biochem Sci* **39**, 612-618 (2014).
19. X. Wan *et al.*, Cascaded amplifying circuits enable ultrasensitive cellular sensors for toxic metals. *Nat Chem Biol* **15**, 540-548 (2019).
- 5 20. C. Y. Huang, J. E. Ferrell, Jr., Ultrasensitivity in the mitogen-activated protein kinase cascade. *Proc Natl Acad Sci U S A* **93**, 10078-10083 (1996).
21. D. Busse *et al.*, Competing feedback loops shape IL-2 signaling between helper and regulatory T lymphocytes in cellular microenvironments. *Proc Natl Acad Sci U S A* **107**, 3058-3063 (2010).
- 10 22. C. Y. Wu, L. J. Rupp, K. T. Roybal, W. A. Lim, Synthetic biology approaches to engineer T cells. *Curr Opin Immunol* **35**, 123-130 (2015).
23. K. T. Roybal *et al.*, Engineering T Cells with Customized Therapeutic Response Programs Using Synthetic Notch Receptors. *Cell* **167**, 419-432 e416 (2016).
- 15 24. K. T. Roybal *et al.*, Precision Tumor Recognition by T Cells With Combinatorial Antigen-Sensing Circuits. *Cell* **164**, 770-779 (2016).
25. L. Morsut *et al.*, Engineering Customized Cell Sensing and Response Behaviors Using Synthetic Notch Receptors. *Cell* **164**, 780-791 (2016).
26. M. Klichinsky *et al.*, Human chimeric antigen receptor macrophages for cancer immunotherapy. *Nat Biotechnol* **38**, 947-953 (2020).
- 20 27. V. Dangles-Marie *et al.*, A three-dimensional tumor cell defect in activating autologous CTLs is associated with inefficient antigen presentation correlated with heat shock protein-70 down-regulation. *Cancer Res* **63**, 3682-3687 (2003).
28. M. Pickl, C. H. Ries, Comparison of 3D and 2D tumor models reveals enhanced HER2 activation in 3D associated with an increased response to trastuzumab. *Oncogene* **28**, 461-468 (2009).
- 25 29. A. E. Cerchiari *et al.*, A strategy for tissue self-organization that is robust to cellular heterogeneity and plasticity. *Proc Natl Acad Sci U S A* **112**, 2287-2292 (2015).
30. A. Lehmann *et al.*, Stability engineering of anti-EGFR scFv antibodies by rational design of a lambda-to-kappa swap of the VL framework using a structure-guided approach. *MAbs* **7**, 1058-1071 (2015).
31. R. C. Roovers *et al.*, A biparatopic anti-EGFR nanobody efficiently inhibits solid tumour growth. *Int J Cancer* **129**, 2013-2024 (2011).
32. D. P. Enot, E. Vacchelli, N. Jacquemet, L. Zitvogel, G. Kroemer, TumGrowth: An open-access web tool for the statistical analysis of tumor growth curves. *Oncoimmunology* **7**, e1462431 (2018).

Acknowledgments: We thank K. T. Roybal, A. Ng and G. Allen for sharing DNA plasmids. We thank the M. Moasser for sharing tumor cell lines for *in vivo* experiments. We thank W. McKeithan for assistance with microscopy data collection and I. Eigl for assistance with biolayer interferometry data collection. We thank A. Li, J. Choe, and members of the Lim Lab for advice and helpful discussions. We thank V. Nguyen and G. Allen for critical reading of this manuscript.

Funding: This work was supported by NIH grants P50GM081879, U54CA244438, R01 CA196277 (W.A.L.), Howard Hughes Medical Institute (W.A.L.), and the UCSF Center for Cellular Construction (DBI-1548297), an NSF Science and Technology Center. R.H.-L. is a Cancer Research Institute Irvington Fellow supported by the Cancer Research Institute. R.H.-L. was a postdoctoral fellow of UC-MEXUS.

Author contributions: R.H.-L. and W.A.L. conceived the project. Experimental plan was implemented by R.H.-L., W.Y., K.A.C., O.A.C., M.L.P., Y.T. and A.G. R.H.-L., K.A.C., and O.A.C. designed and carried out 3D culture experiments supervised by Z.J.G. and W.A.L.

R.H.-L., W.Y., Y.T., A.G. designed and carried out *in vivo* experiments supervised by W.A.L. A.M. and K.S., designed protein expression vectors and provided scFv-GST purified protein constructs. R.H.-L. analyzed all data, R.H.-L., and W.A.L. prepared figures and wrote the manuscript with suggestions from all authors. W.A.L. supervised all aspects of the work.

Competing interests: A provisional patent application has been filed by the University of California related to this work. Z.J.G. is an equity holder in Scribe Biosciences and Provenance Bio.

Data and materials availability: All data are available in the manuscript or supplementary materials. Reagents are available from the corresponding author upon reasonable request. Plasmids from this paper will be made available on Addgene.

Figure Legends

Figure 1. Design of T cells with ultrasensitive antigen density sensing.

A. Ideal therapeutic T cells will distinguish between high antigen density expressing tumor cells and normal cells that express low antigen amounts. A CAR T cell with a standard linear response curve distinguishes poorly between high- and low density cells. Effective discrimination requires a sigmoidal ultrasensitive dose-response curve. **B.** Design of two-step recognition circuit. A synNotch receptor detects antigen (HER2) with low-affinity. This synNotch receptor, when fully activated, induces expression of a high-affinity CAR. The low-affinity synNotch acts as a high antigen density filter, and the high-affinity CAR activates T cell killing and proliferation acting as an amplifier. **C.** Densities of the tumor associated antigen HER2 on engineered stable cell-lines of human leukemia K562. Representative flow cytometry plots ($n=3$). These cell lines can be compared to tumor cell lines (**Fig. S1A**). The average HER2 molecules per cell was measured ($n=3$) as shown in **Fig. S1A**. To construct different HER2 sensing systems, we used a series of anti-HER2 single chain antibodies (scFvs) with affinities spanning a range of over 100-fold. **D.** Binding affinities for anti-HER2 scFvs utilized in this study (See **Fig. S2** for details about sequences and binding affinity measurements). Biolayer interferometry sensograms showing the binding kinetics for human HER2 and immobilized anti-HER2 scFvs. Data are shown as colored lines and the best fit for data to a 1:1 binding model is shown in pink. HER2 concentrations used for binding affinity measurements are indicated.

Figure 2. A two-step low-to-high affinity recognition circuit yields ultrasensitive antigen density sensing.

A. *In vitro* cell killing curves as a function of target cell antigen density, using human primary CD8+ T cells expressing a constitutive CAR of high (scFv $K_d = 17.6$ nM) or low affinity (scFv $K_d = 210$ nM) (top) or a two-step circuit in which the low affinity SynNotch receptor induces expression of either a low or a high affinity CAR (scFv $K_d = 210$ nM synNotch, 17.6 nM CAR)(bottom). For the circuits, lines are fit to a Hill equation (Hill coefficient for each curve is indicated; see **Fig. S4A** for details). For constitutive CARs, lines are drawn based on inspection. The percentage of specific lysis was determined using flow cytometry by counting the number of target cells after 3 days relative to a co-culture of targets in the presence of untransduced T cells (see **Fig. S3C** for gating details). Data are shown as the mean and standard error from the mean ($n=3$). **B.** Representative FACS distributions ($n=3$) for CAR expression and T cell proliferation measured as a function of target cell HER2 density (at 3 days) for T cells expressing a low-to-high affinity recognition circuit. T cell proliferation was only observed at HER2 densities of $>10^5$ (see also **Fig. S4C**). **C.** Model for the mechanism of a two-step circuit expressing a low-affinity synNotch to a high-affinity CAR. In principle, cells with this circuit display two very different responses -- in the presence of a low antigen density target (left) the T cell activity is dominated by the low affinity synNotch and low amounts of a CAR. In the presence of a high antigen density target (right) the expression of a CAR is increased, and the T cell activity is dominated by the high affinity CAR response that activates proliferation and killing. T cell activity is predicted to show a sigmoidal response curve, shown in red, because as antigen density increases, this leads to a gradual increase in CAR expression, transiting between the series of linear response curves shown in purple.

Figure 3. Low-to-high synNotch to CAR circuit: Discrimination between high and low density tumor cancer cell lines and 3D spheroids.

A. Representative FACS distributions ($n=3$) showing the HER2 expression of low and high HER2 cell lines. The HER2 score (as defined by ASCO-CAP scoring guidelines) is shown to the left and the average HER2 density is shown to the right. **B.** Area occupied by target cells as a function of time, normalized by the area occupied by target cells at time 0 (left). Low HER2 density cancer cells (top plot), PC3 (1+ tumor line), or high HER2 density cancer cells (bottom plot), SKOV3 (3+ tumor line), were cultured with human primary CD8⁺ T cells expressing either a two-step circuit low affinity to high affinity CAR (scFv K_d 210 nM synNotch, 17.6 nM CAR) (purple lines) or a high affinity CAR (scFv K_d 17.6 nM) (blue lines). Gray lines correspond to the target area in the presence of untransduced T cells. Solid lines show the average normalized target area and the shades the standard error of the mean ($n=3$ wells, 3 fields of view per well). To the right, representative images of the *in vitro* cell killing experiment. T cells are shown in blue, the low HER2 density cells in green and the high HER2 density cells in red (see Fig. S6 for additional cell lines and Supplemental Movies S1, S2). **C.** Schematics of T cell killing assay of spheroids made of MCF10A cells expressing high or low HER2. A caspase dye (shown in green) was used to track cell death. The FACS distributions show the HER2 expression on MCF10A lines used to make the 3D spheroids, the MCF10A line engineered to express high HER2 is shown in blue, wild type MCF10As that express low levels of HER2 are shown in red. **D.** Representative images of spheroids expressing low (shown in red) or high (shown in blue) HER2 in the presence of untransduced T cells (left) or T cell expressing either a low affinity CAR (middle), or a two-step low-to-high recognition circuit (right). The caspase 3/7 signal is in green and the T cells are labeled in yellow. **E.** Violin plots showing the distributions of mean caspase 3/7 signal per spheroid. The distributions for the low HER2 density spheroids are shown to the left in red and the ones for the high HER2 density spheroids to the right in blue. The mean of the distribution is shown as a white circle, and the number of analyzed spheroids in each case is shown at the bottom. The statistical significance of differences in mean caspase 3/7 signal in each co-culture condition was determined by a Kruskal–Wallis test with Bonferroni's posthoc for multiple comparisons ($ns > 0.05$, * $P < 0.05$, *** $P < 0.0001$). **F.** Schematics of experiment to study the distance-dependence of killing activity of low-to-high circuit T cells in a 3D culture system. High HER2 density spheroids were mixed with large excess of low HER2 density cells and engineered low-to-high circuit T cells. A caspase 3/7 dye was used as a reporter for cell killing. The spheroids and cells were embedded in a thin slab of cell-laden Matrigel to constrain their position along the z-axis. A representative image of a high HER2 spheroid is shown in blue surrounded by low HER2 spheroids, highlighted in red circles, after 3 days of co-culture. The corresponding image for the caspase 3/7 activity is shown below. **G.** Caspase 3/7 activity (fluorescence per pixel within spheroids) is plotted as a function of distance from a high HER2 spheroid, located at the origin. The distances for each low density spheroid to the closest high density spheroid were binned in 50 μm bins and the mean of caspase signal of all spheroids within the bin were computed (on a per pixel basis to account for differences in spheroid size). The gray bars show the mean values of caspase signal for spheroids co-cultured with untransduced T cells; the purple bars show the mean values of caspase signal for spheroids co-cultured with low-to-high circuit T cells. The error bars are the standard error of the mean. A two-sample Kolmogorov-Smirnov test was used to determine the significance of distributions differences ($ns > 0.05$, * $P < 0.05$, *** $P < 0.001$). See Fig.S7 for representative images for each channel showing high density spheroids (blue) surrounded by low HER2 spheroids. T cells were labeled with a yellow cell trace dye.

Fig. 4. Low-to-high synNotch to CAR circuit: Antigen density discrimination in mouse models.

A. Schematics of a two-tumor mouse model experiment to test the efficacy and safety of ultrasensitive antigen density sensing T cells: low affinity synNotch to high affinity CAR circuit (scFv K_d 210 nM synNotch, 17.6 nM CAR). Low and high HER2 tumor cells were injected subcutaneously in the flanks of NSG mice. Engineered primary human CD4+ and CD8+ T cells were injected i.v. at the indicated times after tumor injection. Tumor volume was monitored via caliper measurement over several days after tumor injection. **B.** FACS distributions showing the HER2 expression of cell lines utilized in the experiment. The doses and injection times for tumors and T cells are indicated in the gray box. Tumor volumes of high and low K562 HER2 density cells after treatment with T cells expressing a two-step circuit (low affinity synNotch to high affinity CAR). The high density tumor is shown in dark purple and the low density tumor in pink. The solid lines connect the means and the error bars are the standard error of the mean (n=7). The gray and black dotted lines show the low density and high density tumor volumes after treatment with untransduced T cells, respectively (See **Fig. S10A** for details of control experiment). **C.** Fraction of CD3+ T cells infiltrated in high or low K562 tumors, 7 days after T cell injection. Representative FACS distributions (n=3) showing the CAR expression (mCherry tagged) in CD3+ engineered T cells. **D.** Schematics of a dual tumor mouse model to test the circuit T cell distribution. The doses and injection times for tumors and T cells are indicated in the gray box. Representative image of luciferase expression in dual tumor mice treated with low-to-high circuit T cells, 9 days after T cell injection. Luciferase signal was only detected in the high HER2 tumor, indicating localized expansion (n=2). **E.** Tumor volumes of cancer lines, PC3 (low) and SKOV3 (high) after treatment with T cells expressing a two-step circuit (low affinity synNotch to high affinity CAR) (n=5). The doses and injection times for tumors and T cells are indicated in the gray box. **F.** Tumor volumes of cancer lines, MDA-231 (low) and HCC1569 (high) after treatment with T cells expressing a two-step circuit (low affinity synNotch to high affinity CAR) (n=6). The doses and injection times for tumors and T cells are indicated in the gray box. See **Figs. S9** for more details and individual mouse tumor volume plots. Statistical longitudinal analyses were performed over entire segments of the tumor growth curves using TumGrowth (32). See methods for more details.

Figure 1. Design of T cells with ultrasensitive antigen density sensing.

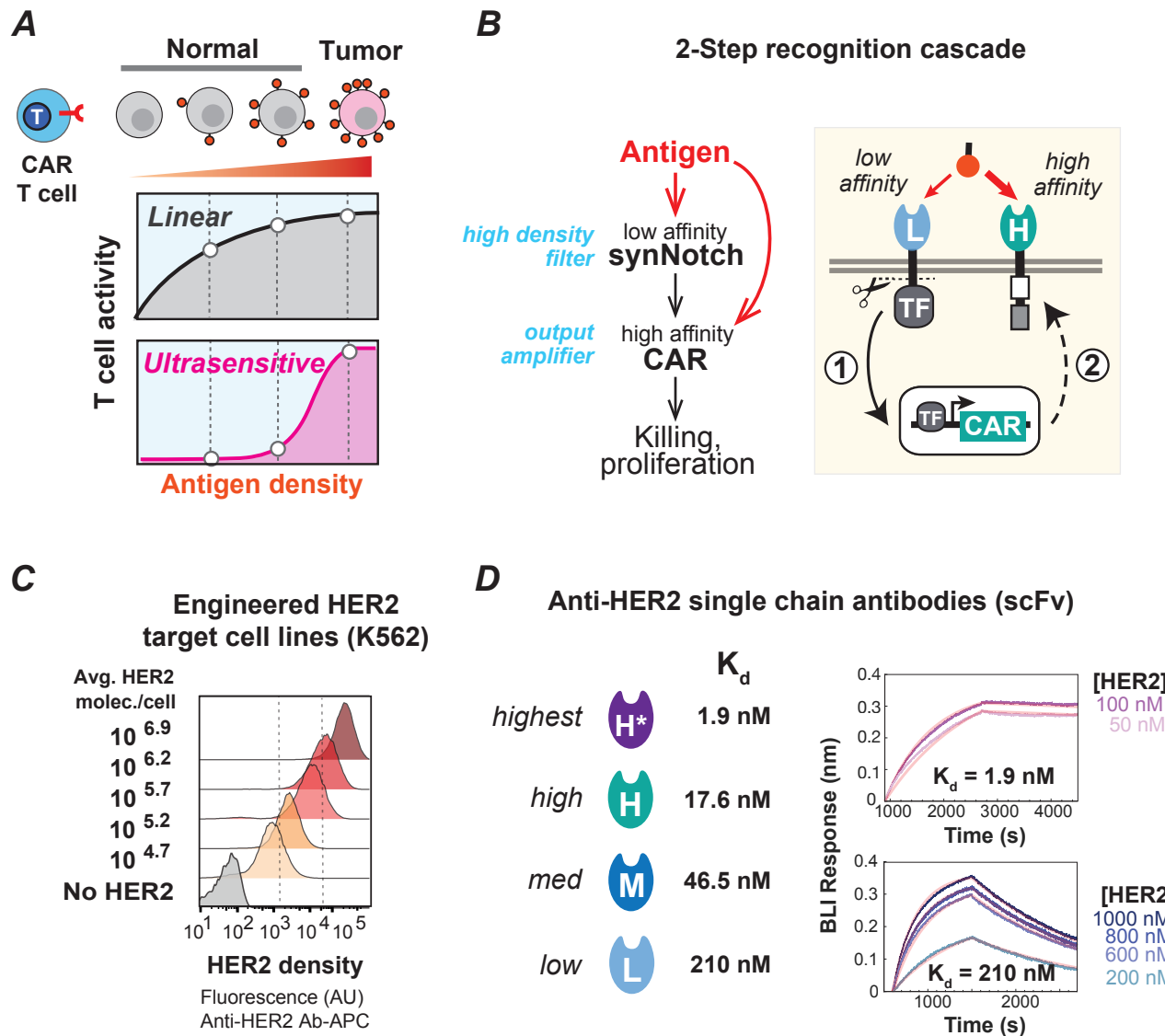


Figure 2. A two-step low-to-high affinity recognition circuit yields ultrasensitive antigen density sensing.

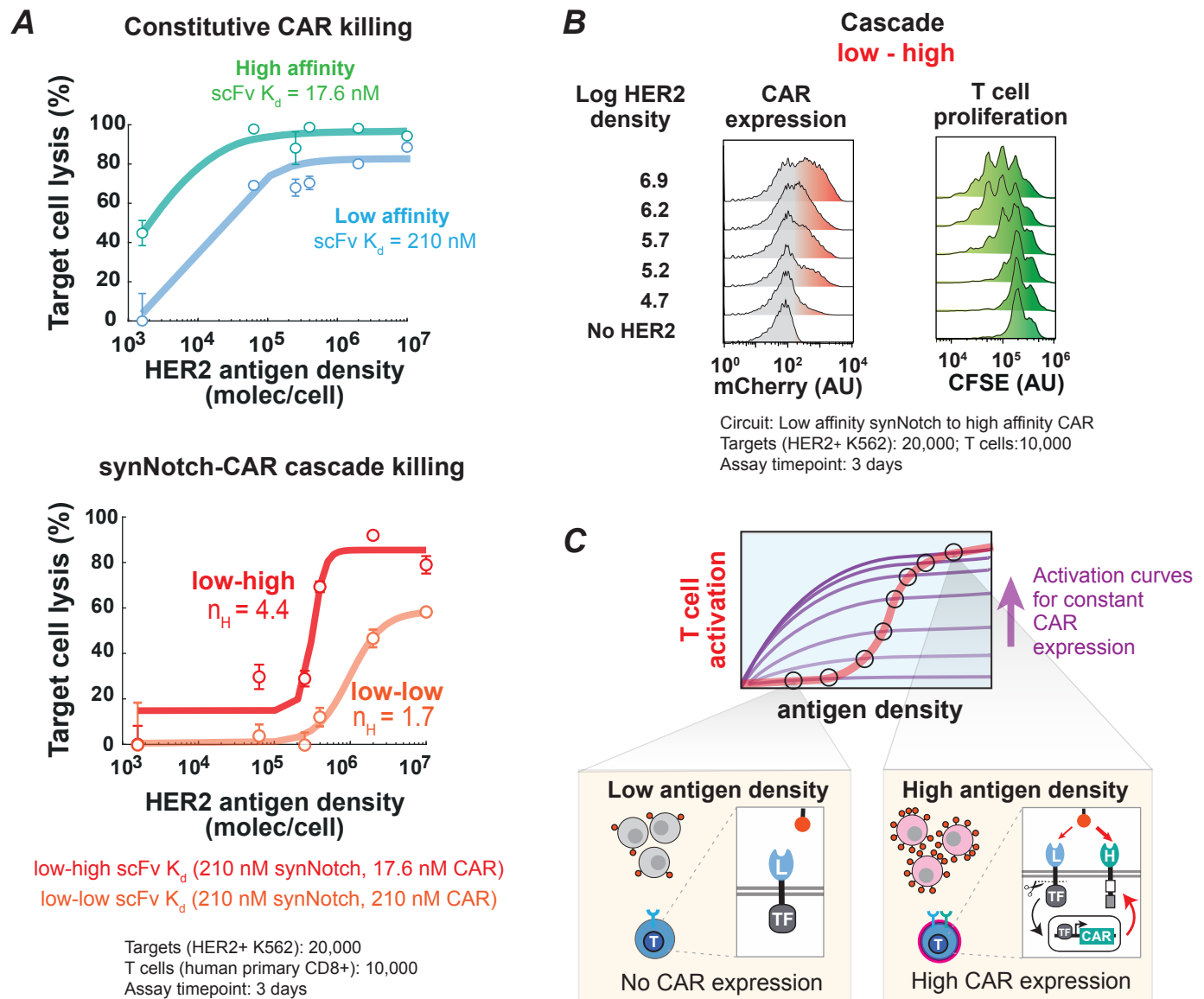


Figure 3. Low-to-high synNotch to CAR circuit: Discrimination between high- and low-density tumor cancer cell lines and 3D spheroids.

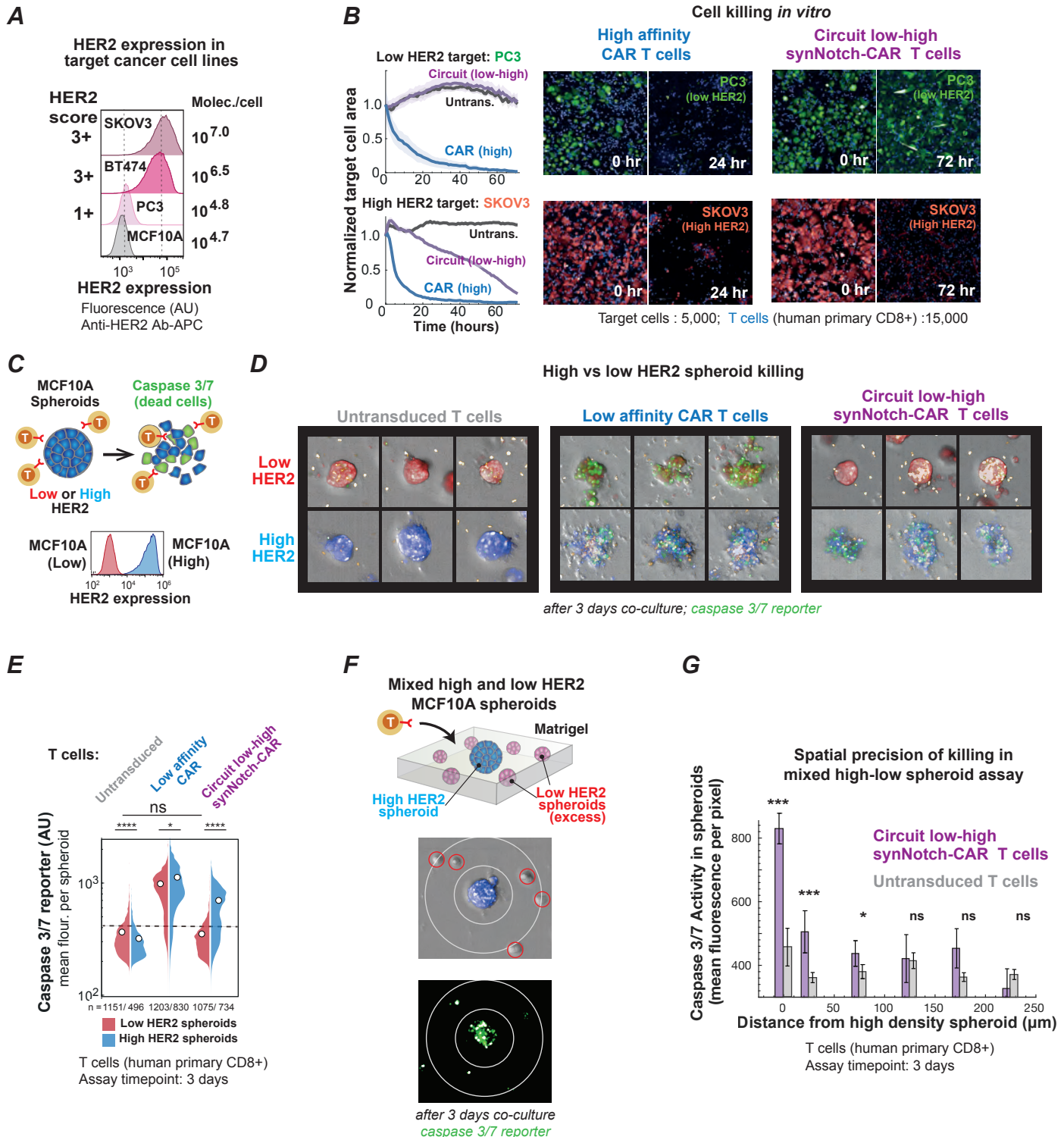
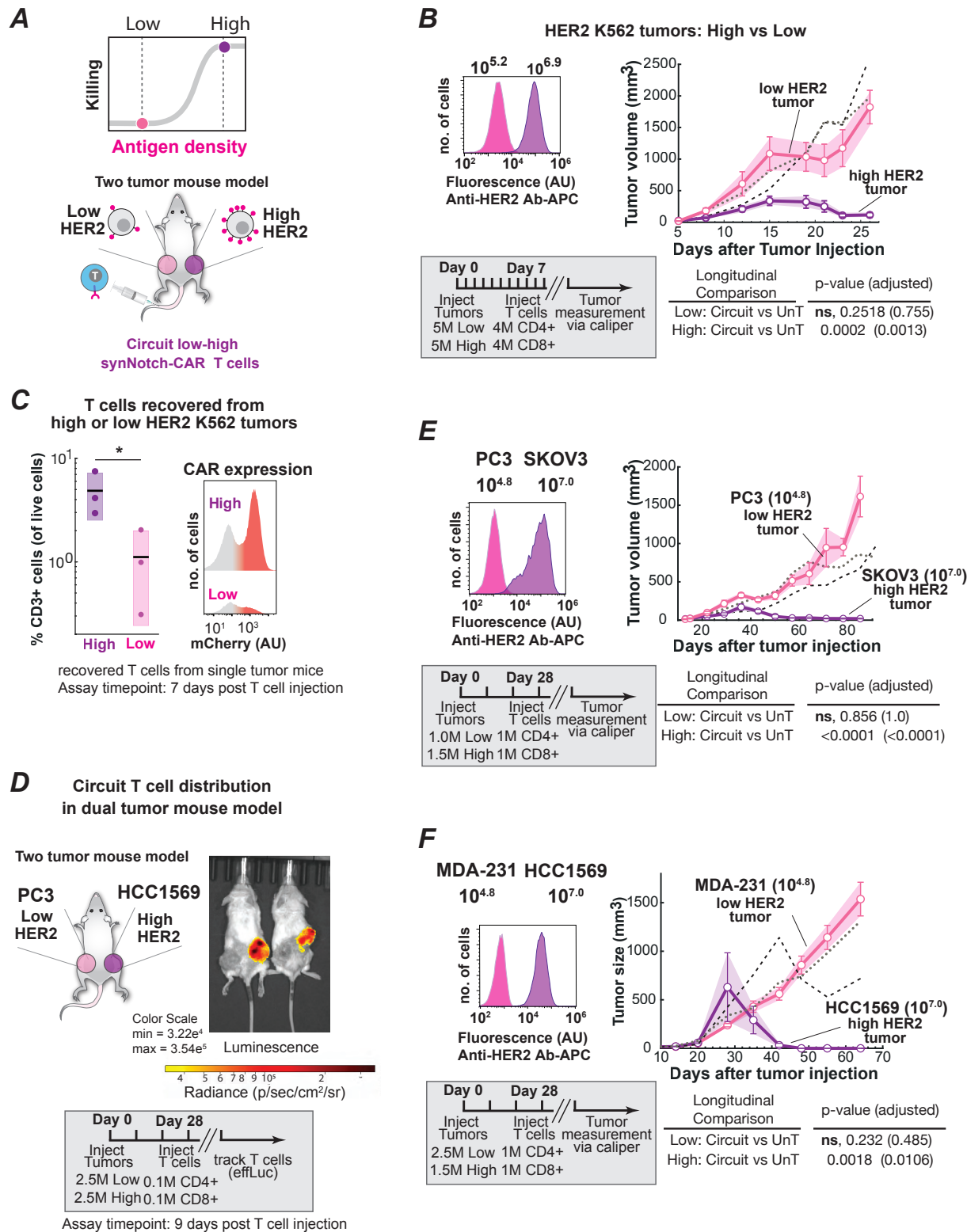


Fig. 4. Low-to-high synNotch to CAR circuit: Discrimination in mouse models.





Supplementary Materials for
T cell circuits that sense antigen density with an ultrasensitive threshold

Rogelio A. Hernandez-Lopez, Wei Yu, Katelyn A. Cabral†, Olivia A. Creasey†, Maria del Pilar Lopez Pazmino, Yurie Tonai, Arsenia De Guzman, Anna Mäkelä, Kalle Saksela, Zev J. Gartner, Wendell A. Lim*.

†These authors contributed equal to this work

Correspondence to: wendell.lim@ucsf.edu

This PDF file includes:

Materials and Methods
Figs. S1 to S13
Captions for Movies S1 and S2

Other Supplementary Materials for this manuscript include the following:

Movies S1 and S2

Materials and Methods

Gene synthesis and cloning

HER2 scFvs: Genes encoding anti-HER2 scFv variants were obtained by gene synthesis as gblocks (Integrated DNA Technologies). Gene fragments were codon optimized for expression in human cells using IDT's website tool.

EGFR scFvs and nanobodies: Similarly, genes encoding anti-EGFR scFv or nanobody variants (30, 31) were obtained by gene synthesis as gblocks (Integrated DNA Technologies).

All constructs were built via in-fusion cloning (Clontech #ST0345) and sequence verified before using them.

Chimeric antigen receptor, SynNotch receptor and response element construct design

Anti-HER2 CARs were built by fusing anti-HER2 scFvs to the hinge region of the human CD8 α chain and transmembrane and cytoplasmic regions of the human 4-1BB, and CD3z signaling domains. CARs were expressed under the control of a spleen focus-forming virus (SFFV) promoter. To obtain low expression levels of CARs, a degron sequence corresponding to the C-terminal region of mouse Ornithine decarboxylase (termed cODC) (EARKAIARVKRESKRIVEDLIMSCAQESAASEKISREAERLIR) was fused to the CD3z signaling domain following a (G₄S)₁ linker.

Anti-HER2 SynNotch receptors were built by fusing anti-HER2 scFvs to the mouse Notch1 minimal regulatory region followed by a Gal4 DNA Binding Domain and the VP64 activation domain, as previously described (23, 24).

All SynNotch receptors and CAR constructs contain an N-terminal CD8a signaling peptide (MALPVTALLPLALLHAAARP) for membrane targeting and a myc-tag (EQKLISEEDL) for determination of surface expression levels. See Morsut, Roybal et al. (25) for details on SynNotch receptor sequence.

The synNotch to CAR circuit constructs were cloned into a single plasmid to avoid copy number variability. The SynNotch receptors were cloned into a modified pHR'SIN:CSW vector and expressed under the control of a pGK promoter. The pHR'SIN:CSW vector was also modified to contain an inducible response element in the same plasmid. Five copies of the Gal4 DNA binding domain target sequence (GGAGCACTGTCCTCCGAACG) were cloned to a minimal CMV promoter. Inducible CAR constructs contain an N-terminal 3X-Flag Tag and C-terminal mCherry protein to determine their protein expression levels.

Engineered K562 HER2 cell lines

A series of engineered HER2 lines were derived from K562 myelogenous leukemia cells (ATCC #CCL-243). K562s were transduced with different amounts of lentivirus to stably express the extracellular and transmembrane region of human HER2 (AA 23-675) fused to a blue fluorescent protein that replaced the endogenous intracellular region. The HER2-BFP construct was expressed under the control of the SFFV promoter. Cells were sorted on an Aria Fusion cell sorter (BD Biosciences) on the basis of HER2 expression and subsequently expanded and frozen at low passage. HER2 levels in each target cell population were determined by staining the cells with anti-HER2 APC (Biolegend 324407); see details below. Overexpression of HER2 is consistent with the amplified levels found in +3, +2 and +1 tumors as scored by ASCO-CAP scoring guidelines (Fig. 1C, Fig. S1A). All engineered K562 cell lines were subcultured in IMDM media supplemented with 10% FBS and gentamicin.

Engineered MCF10A HER2 cell lines

A line overexpressing HER2 was derived from MCF10As. MCF10A is a non-tumorigenic epithelial cell line capable of three-dimensional growth in Matrigel or collagen. MCF10As were transduced with a lentivirus to stably express the extracellular and transmembrane region of human HER2 (AA 23-675) fused to a blue fluorescent protein that replaced the endogenous intracellular region. The HER2-BFP construct was expressed under the control of the SFFV promoter. Cells were sorted on an Aria Fusion cell sorter (BD Biosciences) on the basis of HER2 expression and subsequently expanded and frozen at low passage.

Engineered EGFR cell lines

Similarly, a series of EGFR amplified lines was obtained using a construct that expresses the extracellular region (AA 1-645) of EGFR and transmembrane region of PDGFR (AA 512-561). All cell lines were stained and sorted for expression of transgenes using an anti-EGFR BV786 (BD Bioscience 742606) antibody. Engineered K562-EGFR cell lines were subcultured in IMDM media supplemented with 10% FBS and gentamicin.

Cancer cell lines culturing protocols

Cells were cultured to confluence in the indicated media supplemented with 10% FBS. At each passage, cells were washed with PBS (at 37 °C) and TrypLE (ThermoFisher Scientific 12604021) was added to detach the cells from the flask surface. Flasks were incubated at 37 °C until the cells detached, typically 5 to 10 min. Fresh culture medium was added to quench the TrypLE and cells were resuspended and plated in new flasks and in fresh culture medium. The following cancer cell lines were purchased from the indicated vendors and cultured in the indicated media: PC3 cells (ATCC CRL-1435) were cultured in F-12K medium, SKOV3 cells (ATCC CRL-HTB77) in McCoy's 5a medium, MCF7 cells (ATCC CRL-HTB22) in DMEM medium, BT474 cells (ATCC CRL-HTB20) in RPMI medium and MCF10-A (ATCC CRL-10317) in DMEM/F-12 medium supplemented with 5% horse serum, cholera toxin to a final concentration of 1 ng/mL; human insulin to a final concentration of 10 ug/mL; epidermal growth factor (EGF) to a final concentration of 10 ng/mL; and hydrocortisone to a final concentration of 0.5 ug/mL. MDA-231 and HCC1569 cell lines were gifts of the Moasser Lab (UCSF). MDA-231 cells were cultured in DMEM medium and HCC1569 in RPMI medium.

Determination of protein copy number per cell

Average antigen density per target cell was determined by quantitative flow cytometry. For each of the target antigens or T cell receptors, 1×10^5 cells of each population were stained with the desired antibody: Anti-HER2 APC (Biolegend 324407), Anti-EGFR BV786 (BD Biosciences 742606) or Anti-myc Alexa 647 (CellSignaling 2233S) antibody for 30 min on ice (n=3). Cells were washed twice with PBS and resuspended in PBS for analysis in an Attune NxT Flow Cytometer. The geometric mean of each target population was determined after gating the cells by their size (side scatter and forward scatter region) and selecting the full width at half maximum (FWHM) of the population in the corresponding fluorescent channel. A standard curve was built using Quantum Simply Cellular anti-Mouse IgG beads (Bang Laboratories 815) stained with the same antibody used for the target cells. For each cell line, the number of molecules per cell was determined using the standard curve and the geometric mean of each target population. Similarly, the expression amounts of inducible CAR expression were determined using mCherry flow cytometer calibration beads (Takara Bio 632595).

Primary human T cell isolation and culture

Primary CD4+ and CD8+ T cells were isolated from blood of anonymous donors by negative selection (STEMCELL Technologies #15062 and #15063). T cells were cryopreserved in RPMI-1640 (UCSF cell culture core) with 20% human AB serum (Valley Biomedical, #HP1022) and 10% DMSO. T cells were cultured in human T cell medium (HTCM) consisting of X-VIVO 15 (Lonza #04-418Q), 5% Human AB serum, and 10 mM neutralized N-acetyl L-Cysteine (Sigma-Aldrich #A9165) supplemented with 30 units/mL IL-2 (NCI BRB Preclinical Repository) for all experiments.

Lentiviral transduction of human T cells

Pantropic VSV-G pseudotyped lentivirus was produced by transfecting Lenti-X 293T cells (Clontech #11131D) with a pHR'SIN:CSW transgene expression vector and the viral packaging plasmids pCMVdR8.91 and pMD2.G using Fugene HD (Promega #E2312). Primary T cells were thawed and after 24 hr in culture, were stimulated with Human T-Activator CD3/CD28 Dynabeads (Life Technologies #11131D) at a 1:1 cell:bead ratio. After 48 hr, viral supernatant was harvested and added to primary T cells. T cells were exposed to the virus for 24 hr. At day 5 after T cell stimulation, the Dynabeads were removed. T cells were stained and sorted on an Aria Fusion cell sorter (BD Biosciences) on the basis of myc stain to obtain homogenous receptor expression levels. For the single vectors containing the SynNotch to CAR circuits, T cell transduction efficiency ranged between 10-30% indicating that a single copy of the circuit was inserted. More than 90% of T cells did not express CAR but the few that did (leaky expression) were removed by cell sorting. Untransduced T cells were used to set up the sorting gates but were not sorted as the test articles. T cells were expanded for at least 9 days and cultured at 0.5 million/mL when they were rested and were used for killing assays.

ScFv protein expression and purification

For binding affinity measurements, genes encoding the Anti-HER2 scFv fragments used to build the SynNotch and CAR constructs (including the N-terminal CD8a signaling peptide and the myc-tag) were cloned into a pEBB-GST vector. The pEBB-GST vector was constructed by inserting a GST from *Schistosoma japonicum* transcarboxylase into the polylinker site of the expression vector pEBB. These fusion constructs are under the control of an EF1 α promoter. Expression vectors were used to transiently transfet HEK 293 cells. All proteins were purified from filtered cell supernatants according to the instructions provided with the glutathione-sepharose 4B resin (GE Healthcare). Proteins were dialyzed against PBS after the glutathione elution and flash frozen in small aliquots.

Biolayer interferometry

GST-tagged scFvs were immobilized to an anti-GST capture sensor tip (FortéBio) using an Octet RED384 (FortéBio). The sensors were preconditioned according to the FortéBio protocol and then dipped into a series of concentrations of label free HER2 (Acro biosystems; HE2-H5212) to measure association before being dipped into a well containing only running buffer composed of 1X PBS, 0.05% Tween 20, 0.3 % bovine serum albumin to measure dissociation.

Data were reference subtracted and fit to a 1:1 binding model using Octet Data Analysis Software v11.1 (FortéBio).

In vitro T cell cytotoxicity assessment

CD8+ Primary human T cells expressing either constitutive anti-HER2 CAR or two-step SynNotch-CAR circuits were co-cultured for 72 hr with targets expressing different HER2 densities in complete human T cell medium and placed at 37 °C, 5% CO₂ incubator. In all *in vitro* T cell killing assays against engineered K562 HER2 cells, the T cells were stained with celltrace CFSE dye (Thermo Fisher Scientific C34554) and co-cultured in round bottom 96-well tissue culture plates at the indicated effector to target ratios. The cells were centrifuged for 1 min at 400 x g to favor effector to target interactions, and the cultures were analyzed after 3 days for specific lysis of target tumor cells, T cell proliferation and CAR expression by flow cytometry. Live T cells were identified by the CFSE celltrace dye and live target cells were identified by size after gating for live/dead cells (see **Fig. S3C** for details). The percentage of specific lysis of target cells was determined by comparing the number of target cells alive in the co-culture with engineered T cells compared to treatment with untransduced T cell controls. All flow cytometry was performed using BD LSR II or Attune NxT Flow Cytometers and the analysis was performed in FlowJo software (TreeStar) and Matlab. The following equation was used to calculate the percent of specific lysis.

$$\% \text{ specific lysis} = \left(1 - \frac{\text{Live Targets in coculture with engineered Tcells}}{\text{Live Targets in coculture with UnT T cells}} \right) * 100$$

Curve fitting of *in vitro* T cell cytotoxicity of synNotch to CAR circuits

Data is presented as means ± standard error of the mean (SEM) as indicated in the figure legends. The target cell killing data for the synNotch to CAR circuits was fitted to a four parameter Hill equation using the curve fitting toolbox in Matlab (see **Fig. S4A** for details of the equation and parameters).

Imaging of T cell cytotoxicity- 2D cultures

For all *in vitro* T cell killing of HER2 expressing cancer lines, 5x10³ target cells were stained with a celltrace dye, and were cultured overnight in a flat bottom 384-well tissue culture plate in their indicated medium and placed at 37 °C, 5% CO₂ incubator. After 1 day, 1.5 x 10⁴ T cells were stained and added to the flat bottom 384-well tissue culture plate and the co-cultures were imaged every 3 hours for 3 days. Two or three fields per well were imaged using the 20x objective on a PerkinElmer Opera Phenix High Content Screening System and the images were analyzed using the associated Harmony Office Software. Data was summarized as the sum of the normalized area occupied by target cells and presented as mean ± SEM as shades.

In vitro T cell proliferation and CAR expression with cancer cell lines

For *in vitro* assessment of T cell proliferation and CAR expression with cancer lines, 10x10³ target cells were cultured overnight in a flat bottom 96-well tissue culture plate in their indicated medium and placed at 37 °C, 5% CO₂ incubator. After 1 day, 2.5 x 10⁴ T cells were stained and added to the flat bottom 96-well tissue culture plate. The plates were centrifuged for 1 min at 400 x g to favor effector to target interactions, and cultures were analyzed after 3 days. T cell activation, proliferation and CAR expression were determined by flow cytometry.

In vitro assessment of T cell cytotoxicity – 3D cultures

To assess the killing activity of constitutively expressed anti-HER2 CAR T cells or two-step SynNotch_{low affinity} → CAR_{high affinity} circuit T cells in the context of a three-dimensional culture, we

created spheroids of MCF10A cells using agarose microwells, as previously described (29). Briefly, photolithography was used to create a master wafer with SU-8 microwells of 120 μm diameter, 100 μm height. PDMS micropillar stamps were created from this master by pouring Sylgard 184 (Dow Corning, 10:1 base:crosslinker ratio) over the wafer and baking at 60°C for >3 hours. The PDMS stamps were placed on top of molten agarose (2% weight/volume in PBS (calcium and magnesium free), AllStar Scientific) in glass-bottomed well plates (Cellvis). After the agarose cooled, the PDMS stamps were peeled off, leaving behind 120 μm agarose microwells.

MCF10A cells were re-suspended in PBS + 0.4% EDTA at a density of 2×10^6 cells/mL and added to the well plate containing the agarose microwells. The MCF10As were centrifuged into the agarose microwells at $160 \times g$ for four minutes, the plate was rotated 180 degrees, and then centrifuged a second time. Excess cells that did not occupy the microwells were removed by washing with PBS + EDTA followed by washing with MCF10A media. After overnight culture, the MCF10As in each microwell had coalesced to form spheroidal cell aggregates, termed spheroids.

MCF10A spheroids were removed from the agarose microwells, sedimented with pulsed centrifugation to 20G, and then resuspended in ice-cold Matrigel containing 1×10^6 T cells/mL. The Matrigel + T cell + MCF10A spheroids mixture was plated into Matrigel-coated wells of a glass bottomed 24-well plate (Cellvis). Each well was given Human T cell media containing 30 units/mL IL-2, 20 ng/mL EGF and 2 drops/mL of CellEvent Caspase 3/7 Green Dye (Invitrogen). The Caspase 3/7 dye served as a readout of cell death.

Co-cultures were imaged after 3 days. Several fields and 15 planes, 50 μm apart, per well were imaged using the 5x objective on a PerkinElmer Opera Phenix High Content Screening System and the images were analyzed to segment the spheroids and to determine the caspase 3/7 signal within each spheroid using the associated Harmony Office Software. Data was summarized as the mean caspase fluorescence intensity per spheroid and presented as violin plots. The statistical significance of difference in mean caspase 3/7 signal in each co-culture condition was determined by a Kruskal– Wallis test with Bonferroni’s posthoc for multiple comparisons (ns > 0.05, *P < 0.05, **P < 0.01, ***P < 0.001, ****P < 0.0001)

In vitro assessment of off-target killing radius – 3D Cultures

We estimated the radius of off-target killing of the two-step SynNotch_{low affinity} → CAR_{high affinity} circuit T cells by measuring the Caspase 3/7 signal in HER2-low MCF10A cells surrounding HER2-high MCF10A spheroids. We used the above procedure to make spheroids of high-HER2 MCF10A cells. After overnight culture, the high-HER2 MCF10A spheroids were re-suspended in ice-cold Matrigel containing 1×10^6 T cells/mL and 5×10^5 HER2-low MCF10A cells/mL. Thin slabs of the cell-laden Matrigel were created by adding the cell-laden Matrigel to PDMS flow chambers (dimensions 4 mm x 19 mm x 200 μm) that had been placed onto a hydrophobic glass slide, previously treated with (tridecafluoro-1,1,2,2-tetrahydrooctyl) dimethylchlorosilane (Gelest). After incubation at 37°C for 45 minutes, the PDMS flow chambers containing the cell-laden Matrigel were removed from the slide and placed onto a drop of ice-cold Matrigel in a glass-bottomed plate well. After an additional incubation at 37°C for 45 minutes, media was added (human T cell media + 20 ng/mL EGF + 2 drops/mL Caspase 3/7 Green Dye) and the PDMS flow chambers were removed. The co-cultures were imaged every day up to 3 days with the same conditions described above. The distances for low-HER2 spheroids to the closest high-HER2 spheroid were binned in 50 μm bins and the mean of the caspase signal of all low-

HER2 aggregates within the bin were computed (on a per pixel basis to account for differences in spheroid size). The data was summarized per bin as the mean caspase fluorescence intensity with the standard deviation. The statistical significance between the distributions for the treatment with the circuit T cells and untransduced T cells was determined by a two-sample Kolmogorov-Smirnov test (ns > 0.05, *P < 0.05, **P < 0.01, ***P < 0.001).

In vivo tumor killing and mouse models

All mouse experimental procedures were conducted according to Institutional Animal Care and Use Committee (IACUC)-approved protocols. Female NSG mice were obtained from UCSF breeding core. To evaluate the safety and efficacy of the SynNotch_{low affinity} → CAR_{high affinity} circuit, 6- to 12- week-old animals were inoculated with engineered tumor cells in PBS solution, subcutaneously in the right (high density) and left (low density) flanks, respectively. Single dose treatments consisting of sorted and rested CD4+ and CD8+ (donor matched) engineered or the same number of untransduced T cells were administered intravenously via tail vein in 100 µL of PBS 7 days after tumor injection. Tumor volumes were monitored two times a week via caliper measurements until predetermined IACUC-approved endpoint (hunching, neurological impairments such as circling, ataxia, paralysis, limping, head tilt, balance problems, seizures, tumor volume burden) was reached (n = 5 to 7 mice per group). For experiments with cancer cell lines (PC3, SKOV3, MDA231, HCC1569), cell suspensions in PBS were mixed 1:1 with Matrigel (Corning) and 50 µL were inoculated subcutaneously in the right (high density) and left (low density) flanks, respectively. T cells were administered intravenously via tail vein in 100 µL of PBS at day 28 after tumor injection. Tumor volumes were monitored once a week via caliper measurements until predetermined IACUC-approved endpoint (hunching, neurological impairments such as circling, ataxia, paralysis, limping, head tilt, balance problems, seizures, tumor volume burden) was reached (n = 5 to 7 mice per group). Statistical longitudinal analyses were performed over entire segments of the tumor growth curves using TumGrowth (32). This analysis includes automatic analyses of breakpoints in the tumor growth and outlier detection using Bonferroni-corrected p-values calculated from the residuals. The tumor growth curves were subjected to type II ANOVA and pairwise comparisons across groups, the p-values are reported without and with adjustment by the Holm method.

In vivo Luciferase imaging of SynNotch T cells

6- to 12- week-old animals were inoculated in both flanks with (2.5×10^6 cells) cancer cell lines (low HER2 - PC3 or high HER2 - HCC1569). Cell suspensions in PBS were mixed 1:1 with Matrigel (Corning) and 50 µL were inoculated subcutaneously in the right (high density) and left (low density) flanks, respectively. T cells were administered intravenously via tail vein in 100 µL of PBS at day 28 after tumor injection. A 1:1 mixture of CD4+ and CD8+ (100,000 cells of each T cell type, donor matched) primary human T cells engineered to express constitutively effLuc and the low affinity SynNotch to high affinity CAR circuit were injected intravenously (i.v.) into the tumor-bearing mice (n=2). T cell localization was measured after 9 days with bioluminescence imaging performed using the IVIS 100 (Xenogen) preclinical imaging system. Images were acquired 15 minutes following intraperitoneal (i.p.) injection with 150 mg/kg of D-luciferin (Gold Technology #LUCK-100). Display and adjustment of bioluminescence intensities was performed using the Living image 4.5.4 software (Perkin Elmer), the luminescence scale is indicated in **Fig. 4D**.

In vivo analysis of CAR induction by SynNotch T cells

Experiments to determine the CAR induction *in vivo* were carried out with engineered K562-HER2 cells. Single tumors expressing low- or high-HER2 were implanted into 6- to 12- week-old animals following the same procedures described above. T cells were administered intravenously via tail vein in 100 µL of PBS at the indicated times after tumor injection. A 1:1 mixture of CD4+ and CD8+ (donor matched) primary human T cells engineered to express the low affinity SynNotch to high affinity CAR circuit were injected intravenously (i.v.) into the tumor-bearing mice at the indicated doses. Tumors were harvested at day 7 into RPMI (n=3 per group) and were then minced by razor blade and digested for an hour in RPMI with an enzyme mixture from a human tumor dissociation kit (Miltenyi Biotec #130-095-929) in a tumor gentleMACS dissociator at 37°C to obtain single-cell suspensions. After incubation, the digested tumors were passed over a 70 µm cell strainer and the tumor cells were collected by centrifugation. The cells were then washed with PBS and stained with a LIVE/DEAD Zombie UV dye (BioLegend #423107) for 30 min. After that, cells were stained with α -CD3 APC-eFluor 780 (eBioscience 47-0036-42) to analyze the tumor infiltrating T cells. Expression of mCherry (CAR induction) was assessed in the CD3+ T cell populations with a Fortessa (BD Biosciences) and the analysis was performed in FlowJo software (TreeStar) using the mCherry expression in pre-infused T cells as a control.

Antibodies for antigen expression assessment

Several antibodies were used to assess the antigen expression on different cells types and have been indicated throughout the methods. A summary is indicated in the following list: anti-HER2 APC (Biolegend 324407), anti-EGFR BV786 (BD Bioscience 742606), Anti-myc Alexa 647 (CellSignaling 2233S), α -CD3 APC-eFluor 780 (eBioscience 47-0036-42).

Fig. S1. Determination of antigen density and receptor expression from fluorescence intensity

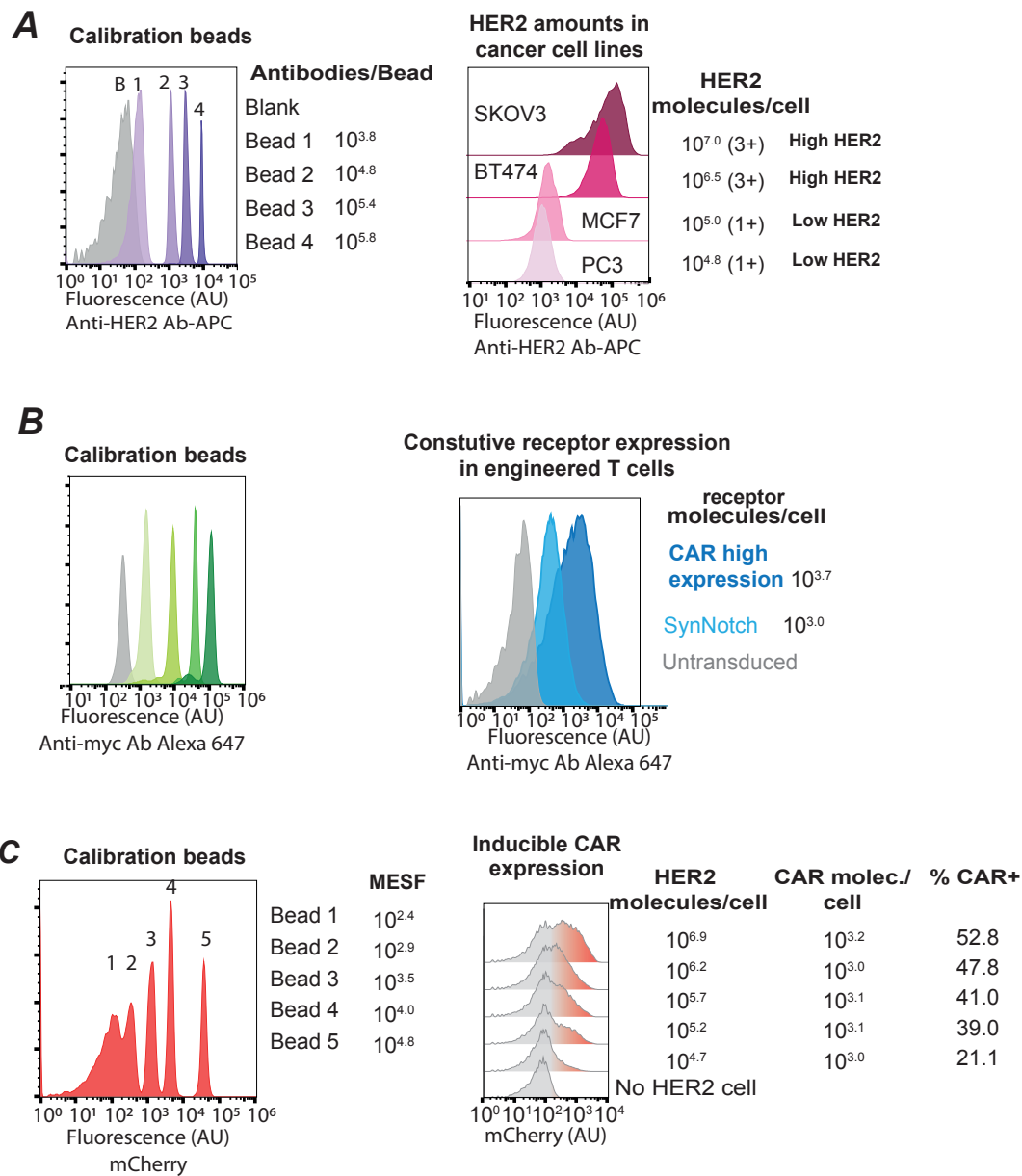


Figure S1. Determination of antigen density and receptor expression from fluorescence intensity.

Antigen density and receptor expression were determined by quantitative flow cytometry. **A.** left: Representative flow cytometry histograms ($n=3$) showing the fluorescence intensity of Quantum Simply Cellular anti-Mouse IgG beads (Bang Laboratories 815) stained with anti-HER2 APC antibody. The manufactured antibody binding capacity of each bead population is indicated to the right in top panel. The geometric mean of each population and a calibration curve built from data shown in the left panel was used to determine the number of HER2 molecules per cell in each population. Right: Representative flow cytometry histograms ($n=3$) showing the fluorescence intensity of cancer cell lines expressing a range of HER2 densities. The density of HER2 molecules/cell and their classification as scored by ASCO-CAP scoring guidelines is shown. **B.** Left: Similar to A for beads stained with anti-myc Alexa 647. Right: Engineered CD8+ human T cells expressing either a constitutive CAR or a SynNotch receptor were stained with anti-myc Alexa 647. The number of receptors per T cell populations was determined as described above. **C.** Left: Representative flow cytometry histograms ($n=3$) of beads showing fluorescence intensity equivalent to the indicated number of soluble mCherry molecules (MESF). Right: Representative histograms ($n=3$) showing the mCherry fluorescence intensity of CD8+ human T cells after 3 days of co-culture with K562 HER2-BFP target cells. The geometric mean of the positive population and the corresponding calibration curve was used to determine the number of induced CAR molecules per cell in each population. The percentage of CAR positive cells was determined using the population comparison platform in FlowJo V10 and it is reported as % SE Dymax. Briefly, it normalizes the data to a unit scale to protect against outliers, and factors in the distribution of the data.

Fig. S2. Protein sequences for anti-HER2 scFvs and their binding affinities

A

4D5_WT_Highest	1	D I Q M T Q S P S S	11	L S A S V G D R V T	21	I T C R A S Q D V N	31	T A V A W Y Q Q K P	41	G K A P K L L I Y S
4D5_Medium		D I Q M T Q S P S S		L S A S V G D R V T		I T C R A S Q D V N		T A V A W Y Q Q K P		G K A P K L L I Y S
4D5_High		D I Q M T Q S P S S		L S A S V G D R V T		I T C R A S Q D V N		T A V A W Y Q Q K P		G K A P K L L I Y S
4D5_Low		D I Q M T Q S P S S		L S A S V G D R V T		I T C R A S Q D V N		T A V A W Y Q Q K P		G K A P K L L I Y S
4D5_WT_Highest	51	A S F L Y S G V P S	61	R F S G S R S G T D	71	F T L T I S S L Q P	81	E D F A T Y Y Y C Q Q	91	H Y T T P P T F G Q
4D5_Medium		A S F L E S G V P S		R F S G S R S G T D		F T L T I S S L Q P		E D F A T Y Y Y C Q Q		H Y T T P P T F G Q
4D5_High		A S F L E S G V P S		R F S G S R S G T D		F T L T I S S L Q P		E D F A T Y Y Y C Q Q		H Y T T P P T F G Q
4D5_Low		A S F L E S G V P S		R F S G S G S G T D		F T L T I S S L Q P		E D F A T Y Y Y C Q Q		H Y T T P P T F G Q
4D5_WT_Highest	101	G T K V E I K R T G	111	S T S G S G K P G S	121	G E G S E V Q L V E	131	S G G G L V Q P G G	141	S L R L S C A A S G
4D5_Medium		G T K V E I K R T G		S T S G S G K P G S		G E G S E V Q L V E		S G G G L V Q P G G		S L R L S C A A S G
4D5_High		G V K V E I K R T G		S T S G S G K P G S		G E G S E V Q L V E		S G G G L V Q P G G		S L R L S C A A S G
4D5_Low		G V K V E I K R T G		S T S G S G K P G S		G E G S E V Q L V E		S G G G L V Q P G G		S L R L S C A A S G
4D5_WT_Highest	151	F N I K D T Y I H W	161	V R Q A P G K G L E	171	W V A R I Y P T N G	181	Y T R Y A D S V K G	191	R F T I S A D T S K
4D5_Medium		F N I K D T Y I H W		V R Q A P G K G L E		W V A R I Y P T N G		Y T R Y A D S V K G		R F T I S A D T S K
4D5_High		F N I K D T Y I H W		V R Q A P G K G L E		W V A R I Y P T N G		Y T R Y A D S V K G		R F T I S A D T S K
4D5_Low		F N I K D T Y I H W		V R Q A P G K G L E		W V A R I Y P T N G		Y T R Y A D S V K G		R F T I S A D T S K
4D5_WT_Highest	201	N T A Y L Q M N S L	211	R A E D T A V Y Y C	221	S R W G G D G F Y A	231	M D V W G Q G T L V	241	T V S S G S
4D5_Medium		N T A Y L Q M N S L		R A E D T A V Y Y C		S R W G G D G F Y A		M D V W G Q G T L V		T V S S G S
4D5_High		N T A Y L Q M N S L		R A E D T A V Y Y C		S R W G G D G F Y A		M D V W G Q G T L V		T V S S G S
4D5_Low		N T A Y L Q M N S L		R A E D T A V Y Y C		S R W G G D G F Y A		M D V W G Q G T L V		T V S S G S

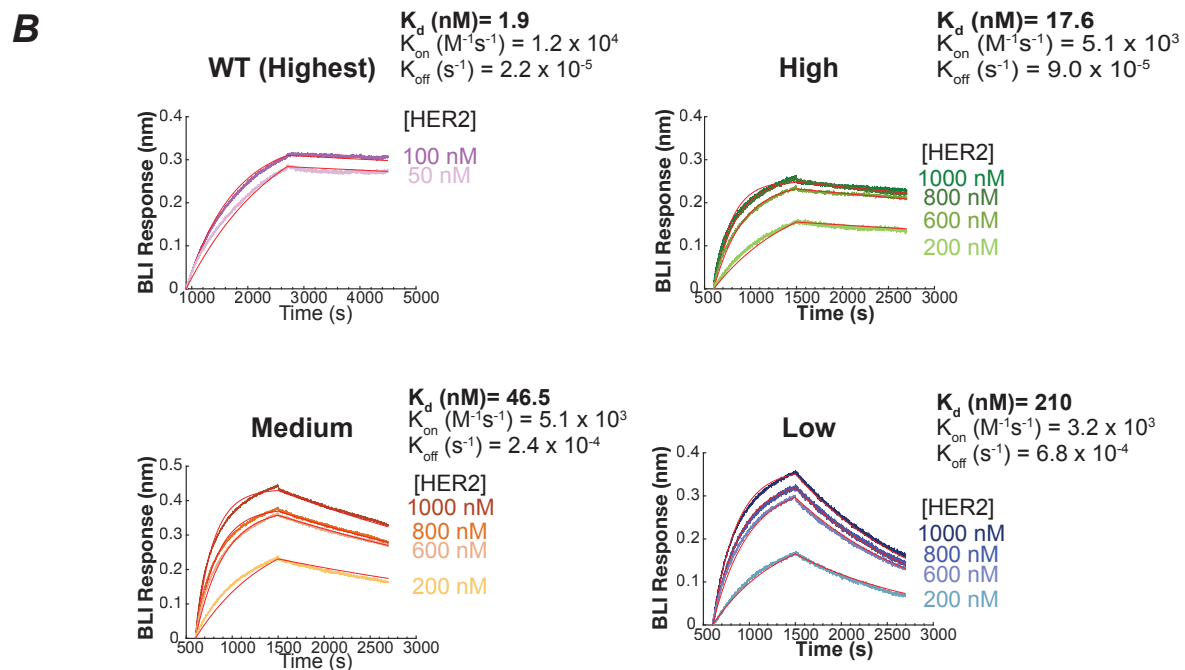


Figure S2. Protein sequences for anti-HER2 scFvs and their binding affinities

A. Sequence alignment of scFvs derived from anti-HER2 4D5 antibody. The WT sequence is labeled as 4D5-WT-Highest and the residues that were mutated to create each variant are indicated in red. **B.** Biolayer interferometry sensograms showing the binding kinetics for human HER2 and immobilized anti-HER2 scFv variants. Data are shown as colored lines and the best fit for data to a 1:1 binding model is shown in red. The binding affinities (K_d), association (K_{on}) and dissociation (K_{off}) constants that resulted from the fit are show. HER2 concentrations utilized for binding affinity measurements are indicated.

Fig. S3. Construct design and flow cytometry gating to quantify killing

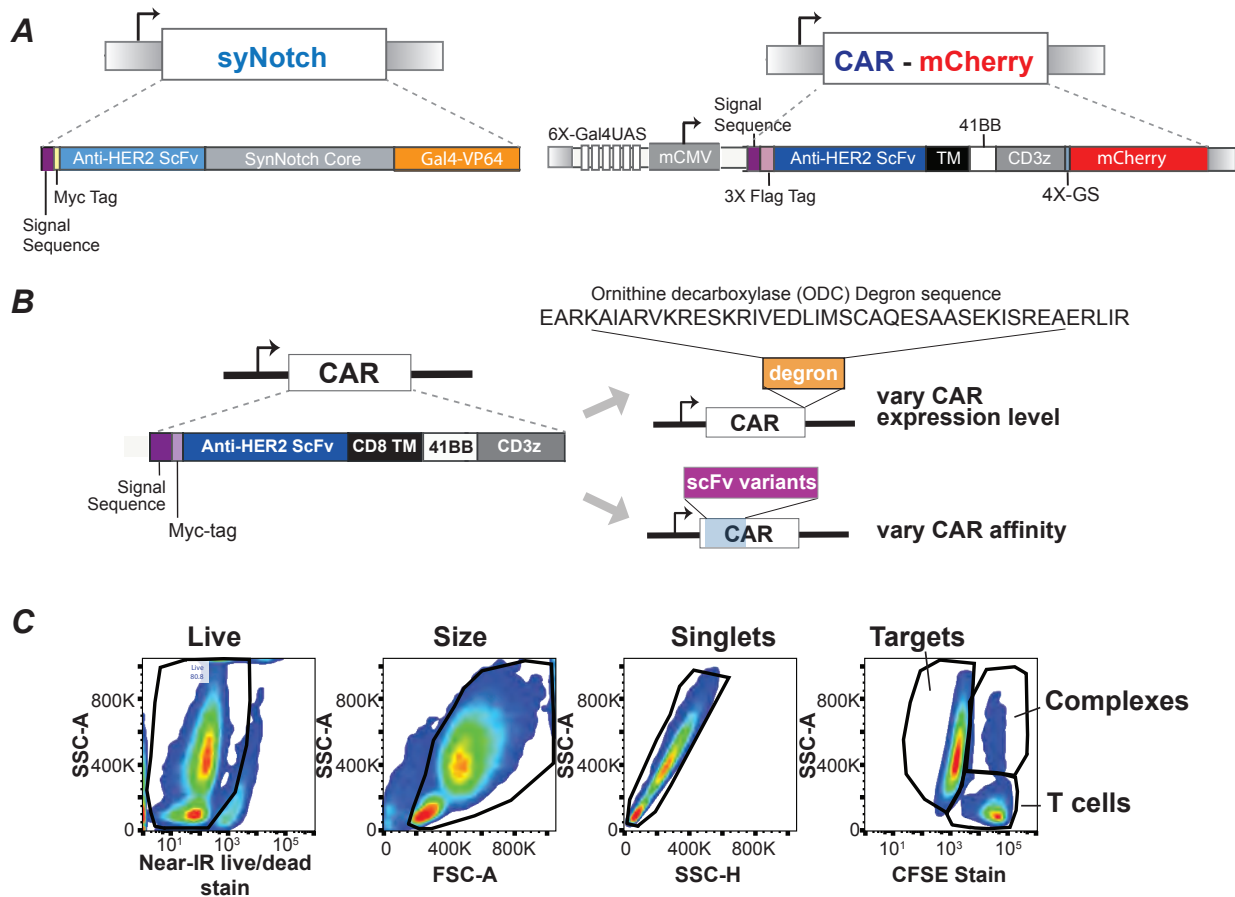


Figure S3. Construct design and flow cytometry gating to quantify killing.

A. Construct design for a two-step SynNotch to CAR circuit used in this study. Both receptors were cloned in a single plasmid to control for copy number. The main domains are indicated and color coded (see methods for details). **B.** Construct design of anti-HER2 CARs used in this study. We obtained T cells expressing varying levels of receptor by fusing a degron tag to the CAR. We altered CAR affinity by changing the scFv domain. The degron sequence corresponds to the C-terminal region of mouse Ornithine decarboxylase (termed cODC) (EARKAIARVKRESKRIVEDLIMSCAQESAASEKISREAERLIR). **C.** Details on gating scheme utilized to analyze *in vitro* killing assays by flow cytometry. Samples were first gated using a viability live-dead cell stain, then using forward and side scattering profiles to select the targets and T cells by size, then single cells, and finally using the CFSE celltrace fluorescence to separate T cells from K562-HER2 targets. T cell-Target complexes were excluded from the analysis.

Fig. S4. Effects of receptor affinity and T cell dosage on two-step circuit function

A

Four parameter Hill equation

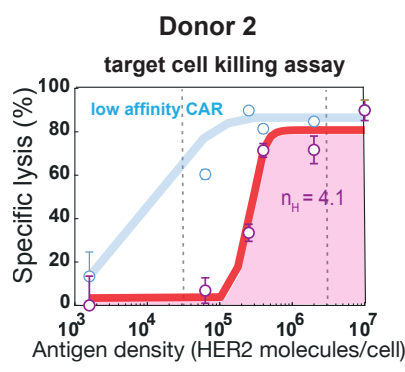
$$\%lysis = k_{min} + \frac{k_{max} - k_{min}}{1 + (\frac{den_{50}}{density})^{n_H}}$$

k_{min} = minimum response
 k_{max} = maximum response
 den_{50} = antigen density for 50% response
 n_H = Hill coefficient

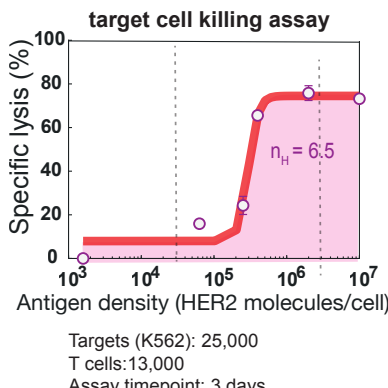
B

Repeat analysis of low-high synNotch-CAR circuit using different donor T cells

Circuit
low-high

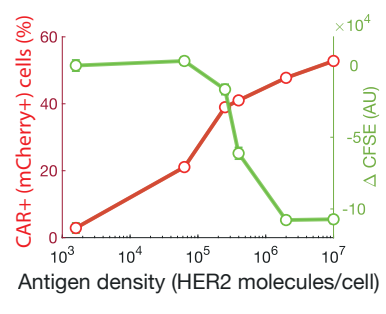


Donor 3



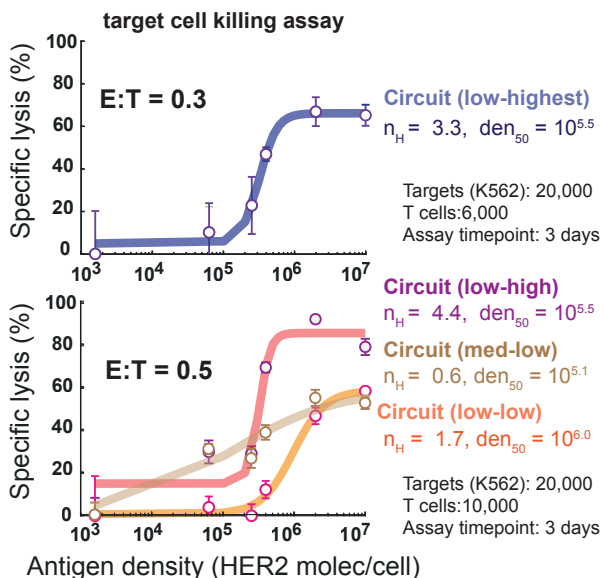
C

Circuit
low-high
Donor 1



D

Ultrasensitivity of other two-step circuits



E

Ultrasensitivity as a function of Effector:Target (E:T) ratio

Circuit
low-high

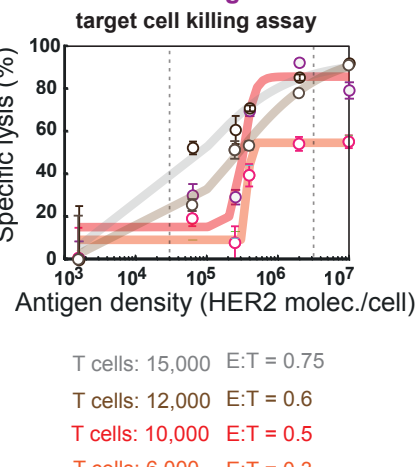
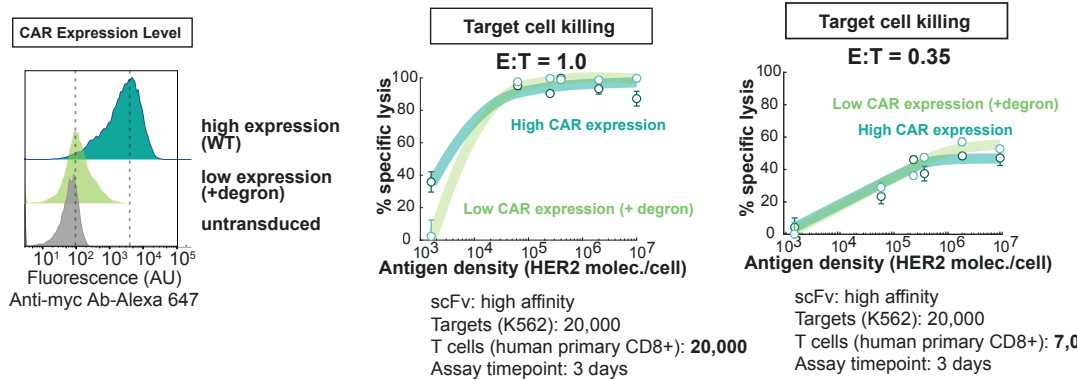


Figure S4. Effects of receptor affinity and T cell dosage on two-step circuit function.

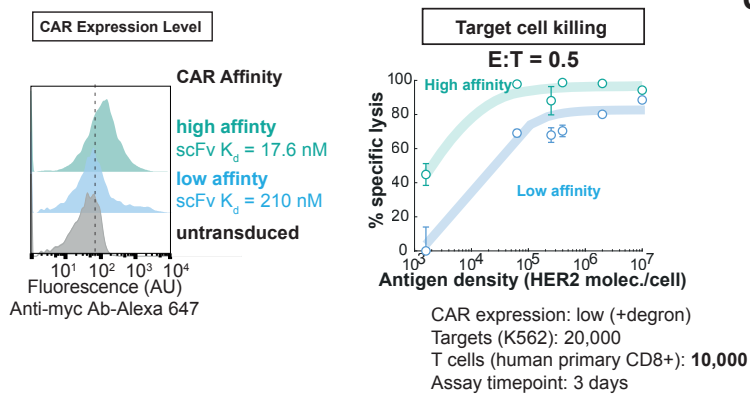
A. Four parameter Hill equation utilized to fit the killing response curves as a function of antigen density of two-step circuits tested in this study. The four parameters are color coded and indicated to the right of the equation. **B.** Target cell killing response curve for T cells expressing a low affinity synNotch to a high affinity CAR circuit from other two different donors of human primary T cells. For donor 2 as a comparison the curve for the constitutive expression of a low affinity CAR is shown. For the circuits transparent lines are fits to a Hill equation; the Hill coefficient for each curve is indicated. For the low affinity CAR, the transparent line is drawn based on inspection. **C.** %CAR+ (mCherry+) cells and dilution of cell trace dye CFSE to assess the CAR expression and T cell proliferation as a function of target cell HER2 density (after 3 days) for T cells expressing a low-to-high affinity recognition circuit (See **Fig. 2B**). The curves as representative of 3 experiments with different T cell donors. **D.** Target cell killing response curves for T cells expressing different two-step circuits variants. A low or medium affinity SynNotch receptor was used in these circuits. Different affinity CAR receptors were tested. The low affinity SynNotch to low affinity CAR circuit showed a higher antigen threshold than other designs (circuit low-low, orange line). The Hill coefficient (n_H) and antigen density for the half maximal activity (den_{50}) values are indicated for each killing curve. **E.** Target cell killing response curves for T cells expressing low affinity SynNotch to high affinity CAR circuit at different effector to target (E:T) ratios. Ultrasensitivity is best observed at low E:T ratios.

Fig. S5. Altering CAR expression level or affinity yields modest linear changes in antigen density sensitivity.

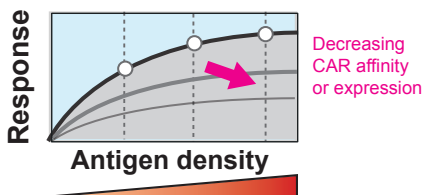
A Vary constitutive anti-HER2 CAR expression level (high affinity)



B Vary constitutive anti-HER2 CAR affinity



C



D T cells expressing either a constitutive low- or high-affinity CAR do not discriminate between low or high HER2 targets in vitro, related to figure 3B.

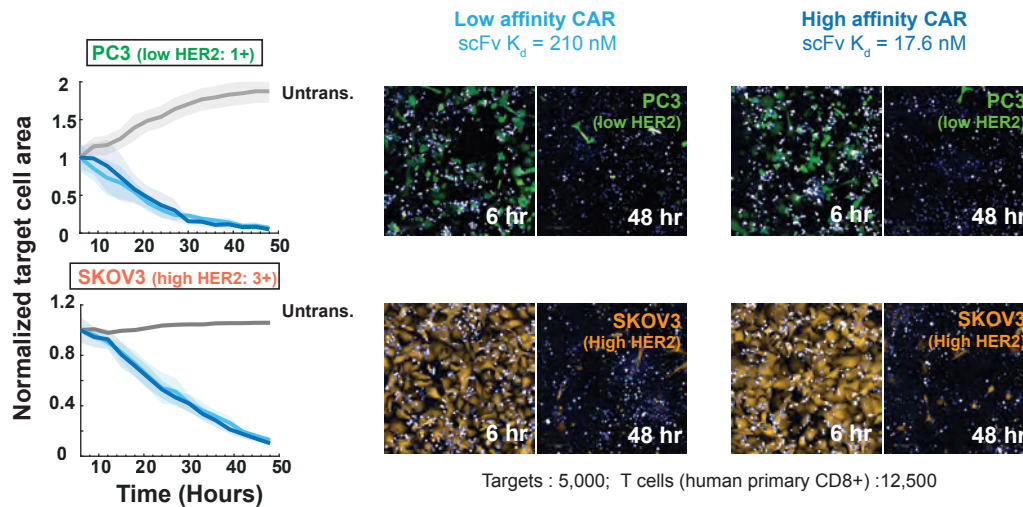
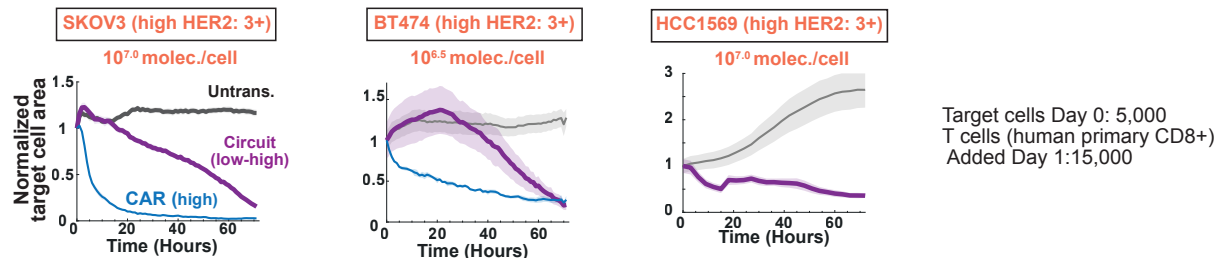


Figure S5. Altering CAR expression level or affinity yields modest linear changes in antigen density sensitivity.

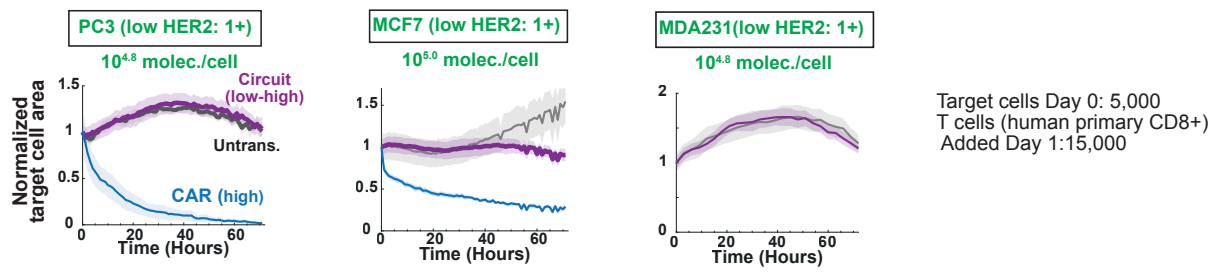
A. Effect of changing CAR expression levels on antigen density dependent cell killing (here we use the high affinity scFv). Representative FACS histograms ($n=3$) for CAR expression distribution in human primary CD8+ T cells, with and without degron tag. Plots on right shows antigen density dependence of target cell killing at two different E:T ratios. **B.** Effect of changing CAR affinity on antigen density dependent cell killing (here we fix low CAR expression - with a degron tag). Representative FACS plots on left show CAR expression distribution of each affinity CAR in human primary CD8+ T cells ($n=3$). Plot on right shows antigen density dependence of target cell killing. Transparent lines are drawn based on inspection. The percentage of specific lysis was determined using quantitative flow cytometry by counting the number of target cells after 3 days relative to a co-culture in the presence of untransduced T cells (see methods for details). **C.** Schematic of effects on changing CAR affinity or CAR expression on antigen density dependent T cell killing response. Decreasing CAR affinity or expression levels leads to linear changes in antigen density response curves. **D.** Area occupied by target cells as a function of time, normalized by the area occupied by target cells at time 6 hours, when the data collection started (left). Low HER2 density cancer cells (top plot), PC3 (1+ tumor line), or high HER2 density cancer cells (bottom plot), SKOV3 (3+ tumor line), were cultured with human primary CD8+ T cells expressing either a high affinity CAR (dark blue lines) or a low affinity CAR (light blue lines). Gray lines correspond to the target area in the presence of untransduced T cells. Solid lines show the average normalized target area and the shades the standard error of the mean ($n=3$ wells, 3 fields of view per well). To the right, representative images of the *in vitro* cell killing experiment. T cells are shown in blue, the low HER2 density cells in green and the high HER2 density cells in orange.

Fig. S6. Low-to-high synNotch to CAR circuit: *In vitro* discrimination with tumor cancer cell lines expressing different HER2 densities.

A Cell killing assays with 3+ HER2 tumor cell lines



B Cell killing assays with 1+ HER2 tumor cell lines



C

Comparison of synNotch-CAR (low-high) circuit T cells vs constitutive low affinity CAR T cells: differential activation by high and low density HER2 tumor cells

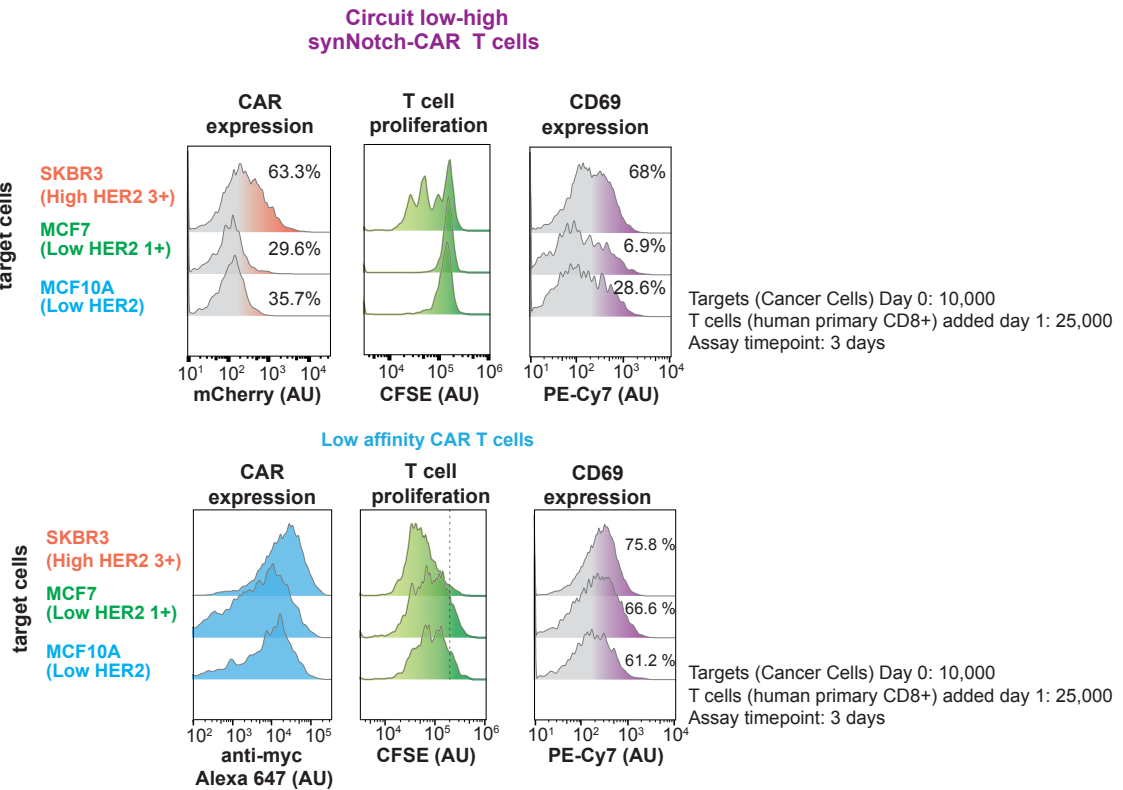


Figure S6. Low-to-high SynNotch to CAR circuit: *In vitro* discrimination with tumor cancer lines expressing different HER2 densities.

A. Cell killing assays with HER2 tumor cell lines (3+). Normalized area occupied by target cells over time. Cancer lines overexpressing HER2 were co-cultured with human primary CD8+ T cells expressing either a two-step circuit (low affinity synNotch to high affinity CAR) (purple lines) or a high affinity CAR (blue lines). Gray lines correspond to the target cell area in the presence of untransduced T cells. Solid lines show the average target area and shaded areas show the standard error of the mean ($n=3$). The mean HER2 density is indicated for each cancer line. **B.** Cell killing assays with HER2 tumor cell lines (1+). Normalized area occupied by target cells over time. Cancer lines expressing low HER2 amounts were co-cultured with human primary CD8+ T cells expressing either a two-step circuit (low affinity synNotch to high affinity CAR) (purple lines) or a high affinity CAR (blue lines). Gray lines correspond to the target cell area in the presence of untransduced T cells. Solid lines show the average target area and shaded areas show the standard error of the mean ($n=3$). The mean HER2 density is indicated for each cancer line. **C.** Representative FACS plots ($n=3$) of CAR expression, T cell proliferation and CD69 expression for T cells co-cultured with cancer cell lines expressing high and low HER2 densities. The histograms in the top row correspond to the two-step circuit low affinity synNotch to high affinity CAR T cells. The histograms in the bottom row correspond to a constitutive low affinity CAR.

Fig. S7. T cells expressing a low-to-high ynNotch-CAR circuit discriminate high and low HER2 spheroids and do not kill low density HER2 spheroids that are far apart from high density HER2 spheroids.

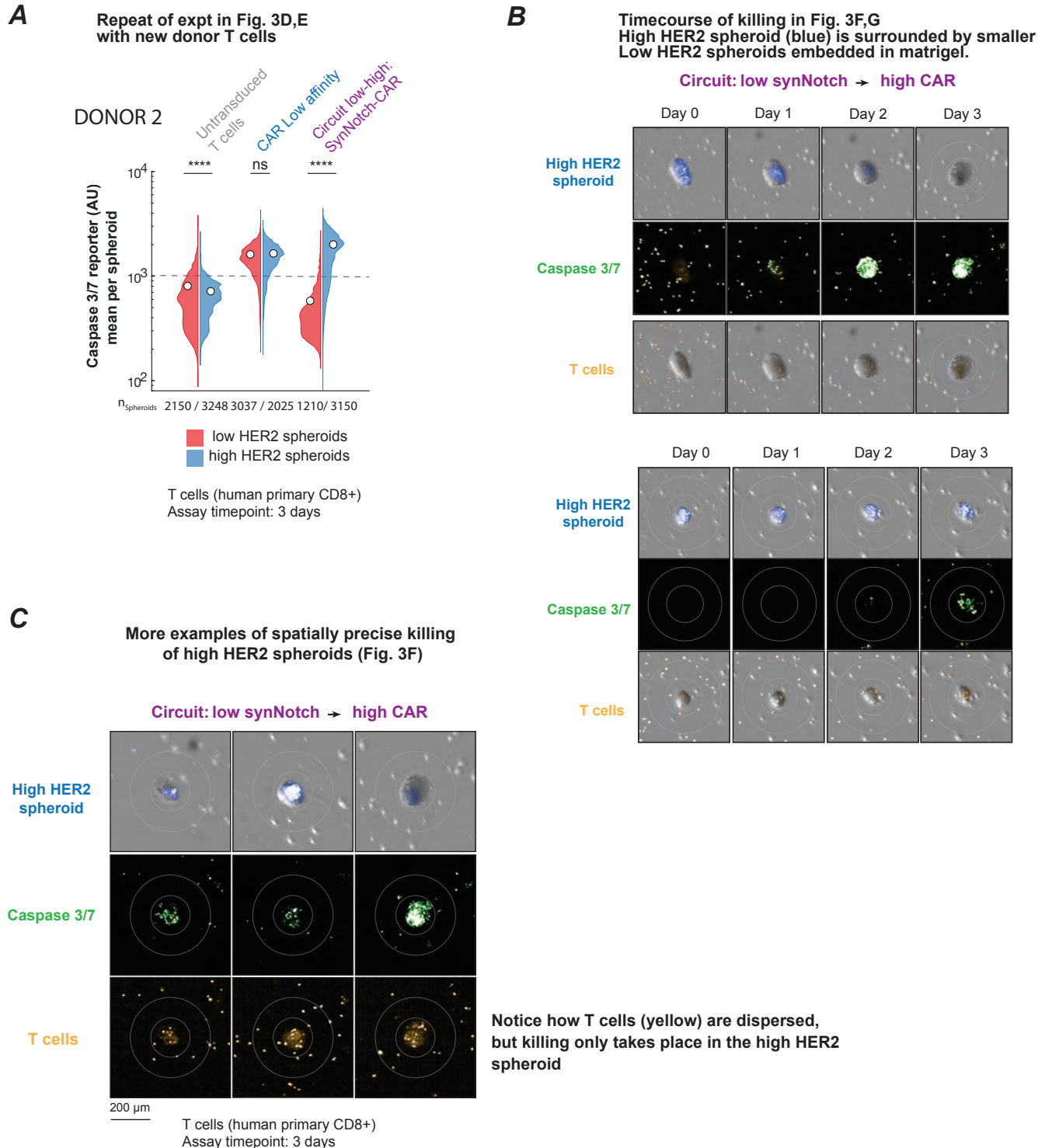
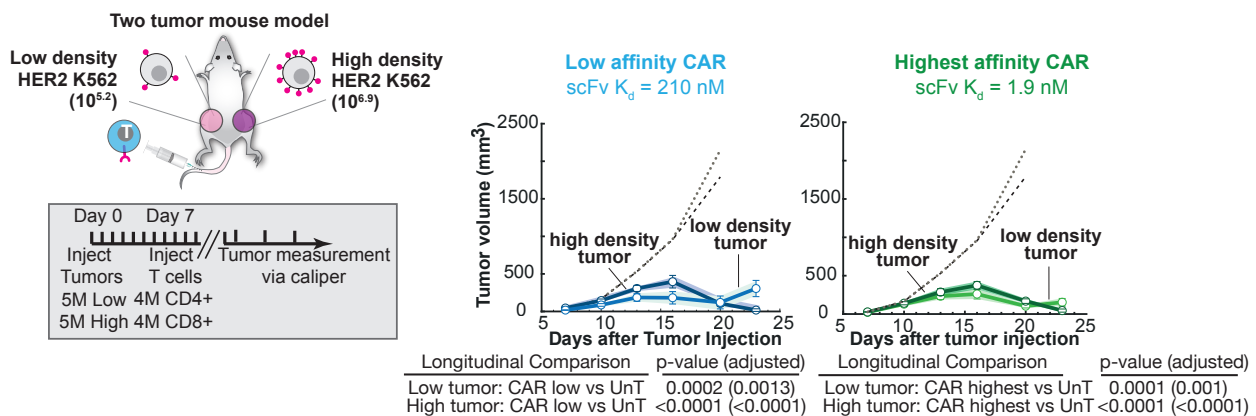


Figure S7. T cells expressing a low-to-high synNotch-CAR circuit discriminate high and low HER2 spheroids and do no kill low density HER2 spheroids that are far apart from high density HER2 spheroids.

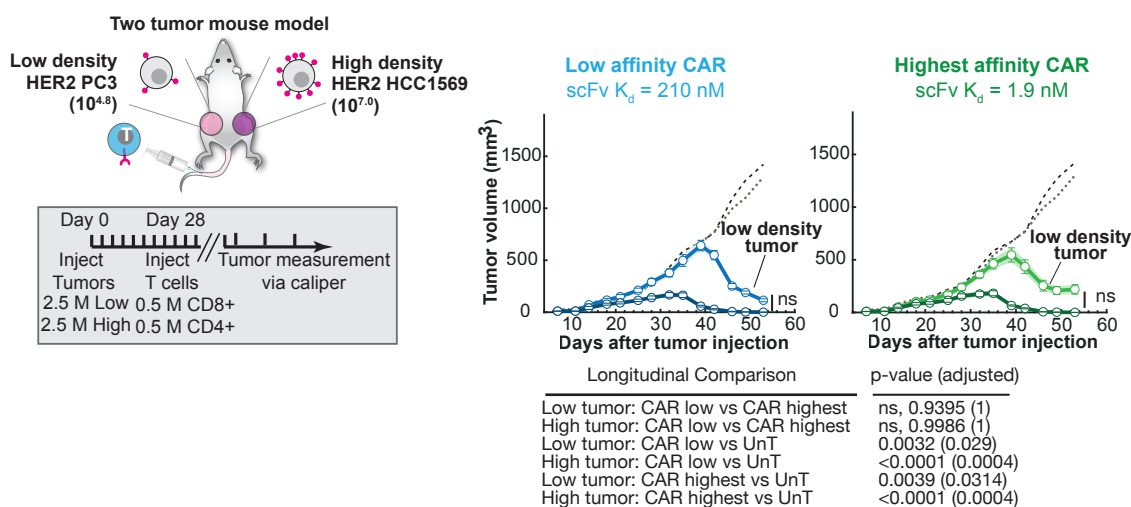
A. Violin plots showing the distributions of mean caspase 3/7 signal per spheroid, related to **Fig. 3D,E**. Results with a different donor T cells. The distributions for the low HER2 density spheroids are shown to the left in red and the ones for the high HER2 density spheroids to the right in blue. The mean of the distribution is shown as a white circle, and the number of analyzed spheroids in each case is shown at the bottom. The statistical significance of differences in mean caspase 3/7 signal in each co-culture condition was determined by a Kruskal–Wallis test with Bonferroni’s posthoc for multiple comparisons (ns > 0.05, *P < 0.05, ***P<0.0001). **B.** Representative projection images of time course killing experiment show in **Fig. 3F,G**. High density spheroids (blue) are surrounded by low HER2 spheroids. T cells were labeled with a yellow cell trace dye, the caspase 3/7 signal is shown in green. **C.** Representative projection images for mixed spheroid killing assay after 3 days of coculture. Each channel showing high density spheroids (blue) surrounded by low HER2 spheroids. T cells were labeled with a yellow cell trace dye. Notice how the caspase 3/7 signal is localized only in the high HER2 spheroid, the T cells are dispersed but enriched in the high HER2 spheroids.

Fig. S8. T cells expressing a constitutive CAR (either low- or high-affinity) do not effectively discriminate between high and low HER2 tumors implanted in mice

A Constitutive CAR T cells clear both high and low density HER2 K562 tumors (bilateral tumors)



B Constitutive CAR T cells clear both high and low density HER2 tumor cell lines (bilateral tumors)



C Constitutive CAR T cells clear both high and low density HER2 tumor cell lines (comparison of single tumor mice)

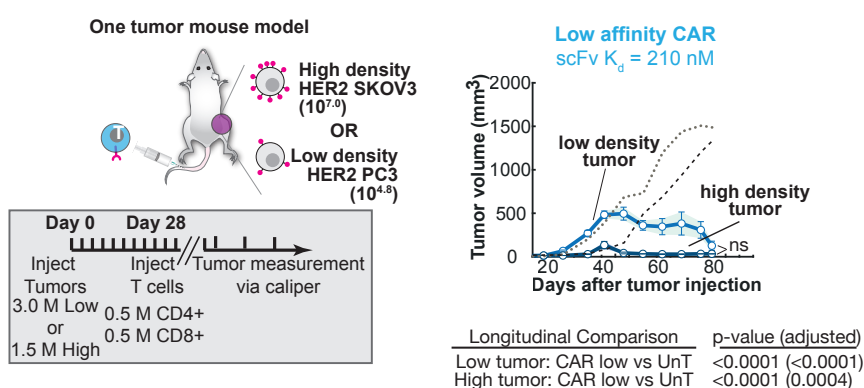
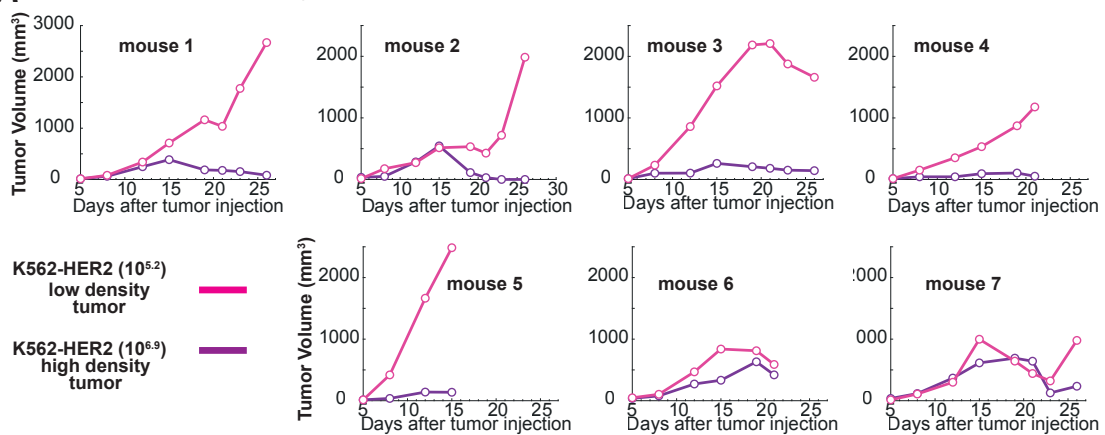


Figure S8. T cells expressing a constitutive CAR (either low- or high affinity) do not effectively discriminate between high and low HER2 tumors implanted in mice.

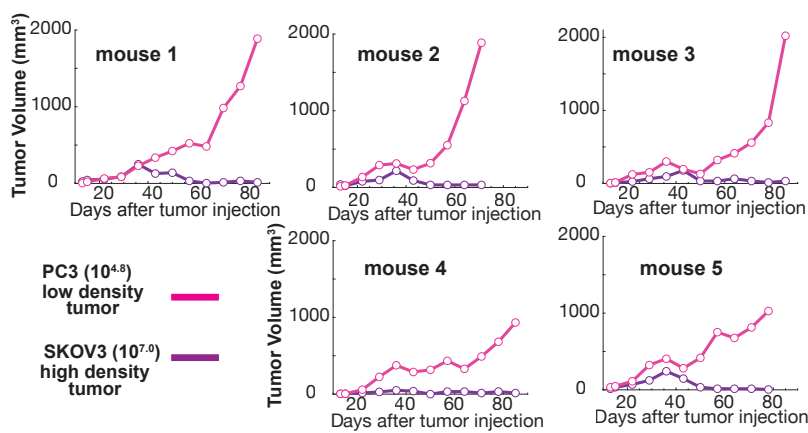
A. Schematic of a two-tumor mouse model experiment. Low and high engineered K562-HER2 tumor cells were injected subcutaneously in the flanks of N.S.G. mice. Engineered primary human CD4+ and CD8+ T cells were injected i.v. 7 days after tumor injection. Tumor volume was monitored via caliper measurement over several days after tumor injection. The dark blue line corresponds to the high HER2 K562 tumor whereas the light blue lines corresponds to the low HER2 K562 tumor after treatment with constitutive low affinity CAR ($\text{scFv } K_d = 210 \text{ nM}$) ($n=8$). The dark green line corresponds to the high HER2 K562 tumor whereas the light green line corresponds to the low HER2 K562 tumor after treatment with constitutive highest affinity CAR ($\text{scFv } K_d = 1.9 \text{ nM}$) ($n=8$). The gray and black dotted lines show the low density and high density mean tumor volumes after treatment with untransduced T cells ($n=8$). **B.** Similar experiment than above but for mice subcutaneously implanted with dual tumors of cancer cell lines expressing low (PC3) or high (HCC1569) HER2 amounts. The blue lines correspond to the treatment with a low affinity CAR ($n=6$), the green lines to the highest affinity CAR ($n=6$) and the gray and black dotted lines correspond to the treatment with untransduced T cells ($n=6$). The doses and injection times for tumors and T cells are indicated in the gray box. **C.** Schematic of a one-tumor mouse model experiment. Low (PC3) or high (SKOV3) HER2 tumor cells were injected subcutaneously in the flanks of N.S.G. mice. Engineered primary human CD4+ and CD8+ T cells were injected i.v. 28 days after tumor injection. Tumor volume was monitored via caliper measurement over several days after tumor injection. The dark blue line corresponds to the high HER2 (SKOV3, $n=5$) tumor whereas the light blue line corresponds to the low HER2 (PC3, $n=6$) tumor after treatment with constitutive low affinity CAR. The gray and black dotted lines show the low density ($n=6$) and high density ($n=6$) mean tumor volumes after treatment with untransduced T cells respectively. For more information about control experiments with untransduced T cells see **Fig. S10D-F**. Statistical longitudinal analyses were performed over entire segments of the tumor growth curves using TumGrowth (32). See methods for more details.

Fig. S9. Tumor volume measurements for individual mice treated with T cells expressing low-affinity synNotch to high-affinity CAR circuit.

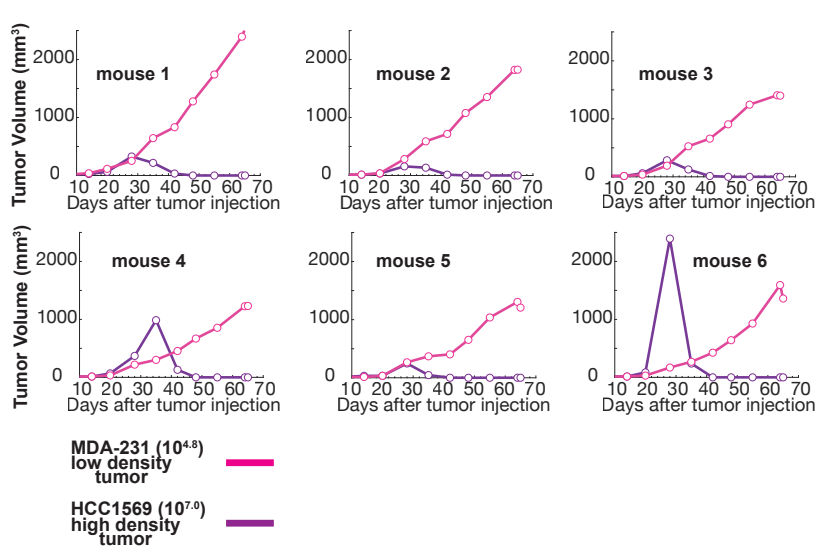
A Individual mouse data for Fig. 4B



B Individual mouse data for Fig. 4E



C Individual mouse data for Fig. 4F



D

Effect of circuit on single low density HER2 tumor

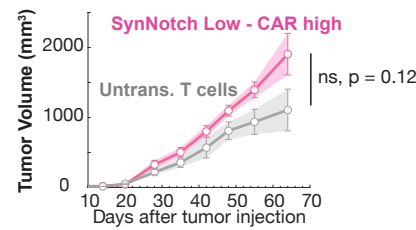
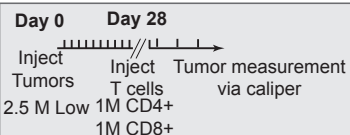


Figure S9. Tumor volume measurements for individual mice treated with T cells expressing low affinity synNotch to high affinity CAR circuit.

A. Tumor volume data for individual mice treated with T cells expressing a low affinity SynNotch to high affinity CAR circuit. The dark purple lines correspond to the high HER2 K562 tumor whereas the light pink lines correspond to the low HER2 K562 tumor (See **Fig. 4B**). **B.** Tumor volume data for individual mice treated with T cells expressing a low affinity synNotch to high affinity CAR circuit. The dark purple lines correspond to the high (SKOV3) tumor whereas the light pink lines correspond to the low (PC3) tumor (See **Fig. 4E**). **C.** Tumor volume data for individual mice treated with T cells expressing a low affinity synNotch to high affinity CAR circuit. The dark purple lines correspond to the high (HCC1569) tumor whereas the light pink lines correspond to the low (MDA-231) tumor (See **Fig. 4F**). **D.** Schematic of a one-tumor mouse model experiment. Low (MDA-231) HER2 tumor cells were injected subcutaneously in the flank of N.S.G. mice. Engineered primary human CD4+ and CD8+ T cells were injected i.v. 28 days after tumor injection. The light pink line corresponds to the mean tumor volume for mice treated with T cells expressing a low affinity synNotch to high affinity CAR circuit ($n=4$). The gray line shows the mean tumor volume after treatment with untransduced T cells ($n=5$). Statistical longitudinal analyses were performed over entire segments of the tumor growth curves using TumGrowth (32). See methods for more details.

Fig. S10. Control experiments for Fig. 4 and Fig. S8: Tumor volume growth measurements for mouse models treated with untransduced T cells.

These curves represent the dotted lines shown in Fig. 4.

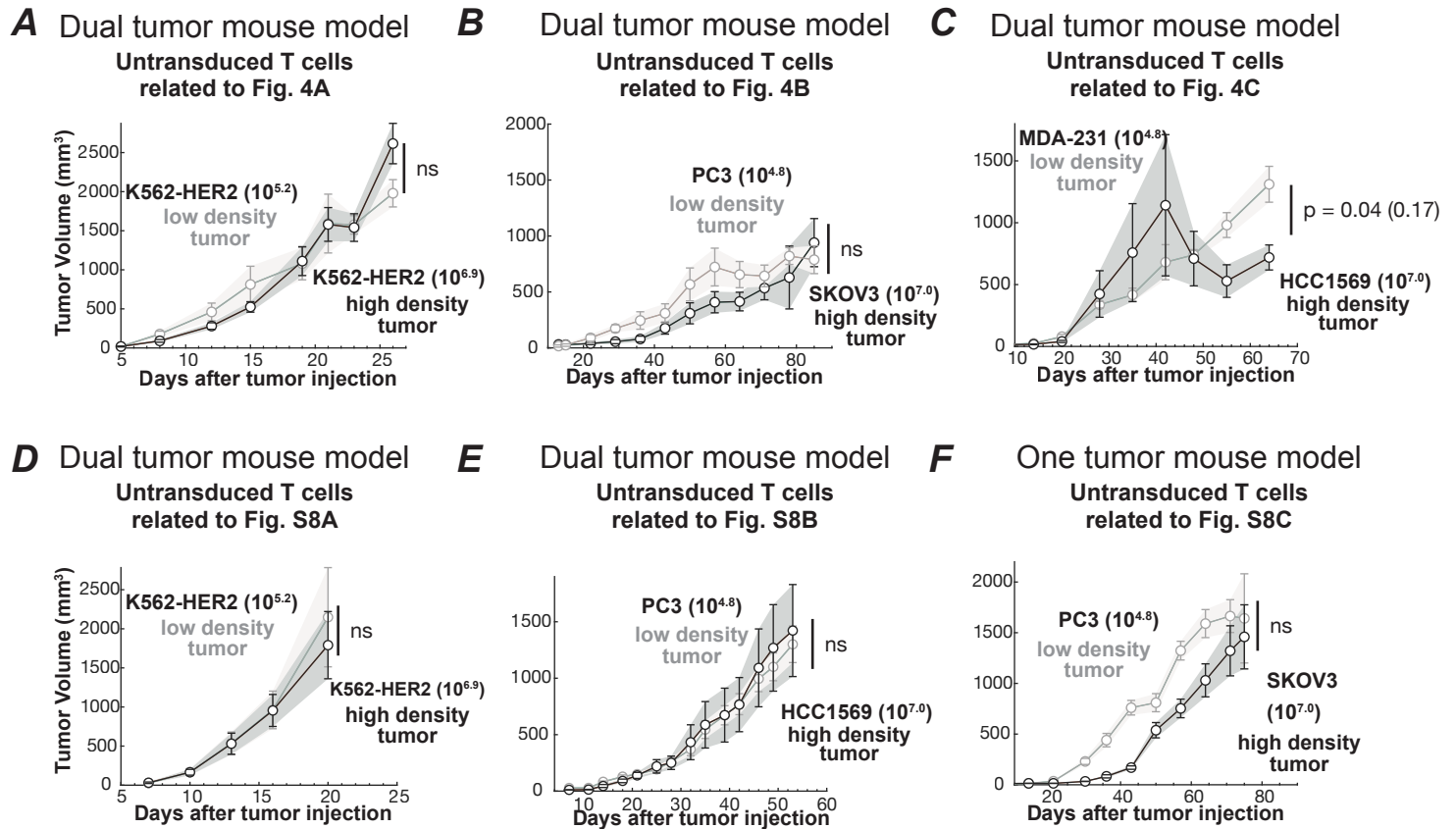


Figure S10. Control experiments for Fig. 4 and Fig. S8: Tumor volume growth measurements for mouse models treated with untransduced T cells.

A. Tumor volume measurement for low- and high HER2 engineered K562 cell lines after treatment with untransduced T cells (n=7), related to Fig. 4A. **B.** Tumor volume measurement for low (PC3) and high (SKOV3) HER2 cancer lines after treatment with untransduced T cells (n=5), related to Fig. 4B. **C.** Tumor volume measurement for low (MDA-231) and high (HCC1569) HER2 cancer lines after treatment with untransduced T cells (n=6), related to Fig. 4C. **D.** Tumor volume measurement for low- and high HER2 engineered K562 cell lines after treatment with untransduced T cells (n=8), related to Fig. S8A. **E.** Tumor volume measurement for low (PC3) and high (HCC1569) HER2 cancer lines after treatment with untransduced T cells (n=6), related to Fig. S8B. **F.** Tumor volume measurement for low (PC3, n=6) and high (SKOV3, n=6) HER2 cancer lines after treatment with untransduced T cells, related to Fig. S8C. Statistical longitudinal analyses were performed over entire segments of the tumor growth curves using TumGrowth (32). See methods for more details.

Fig. S11. Gating strategy to measure intratumoral low-high synNotch-CAR T cells expansion and CAR induction in mouse models

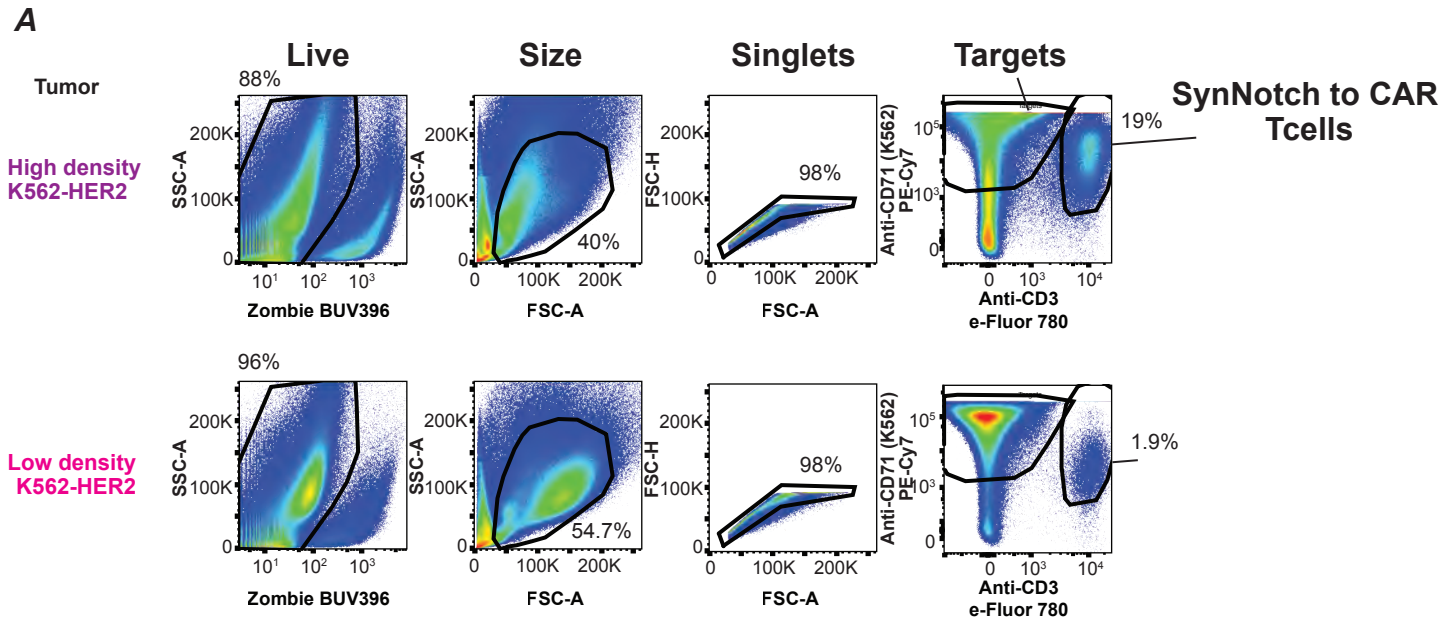


Figure S11. Gating strategy to measure intratumoral low-high synNotch-CAR T cells expansion and CAR induction in mouse models.

A. Details on gating scheme utilized to analyze *in vivo* expansion and CAR induction by flow cytometry. Single cell suspension samples were first gated using a UV zombie live-dead cell stain dye, then using forward and side scattering profiles to select single cells and finally using an anti-CD3 stain to identify low-high synNotch-CAR T cells. The mCherry signal (CAR expression) was measured for the CD3+ T cells. The FACs plots are representative of engineered low and high HER2 K562 tumor samples (n=3 of each).

Fig. S12. Low-affinity synNotch to high-affinity CAR circuit shows effective high vs low HER2 density tumor discrimination over at least 5-fold range of starting effector to target ratios (related to Fig. 4B).

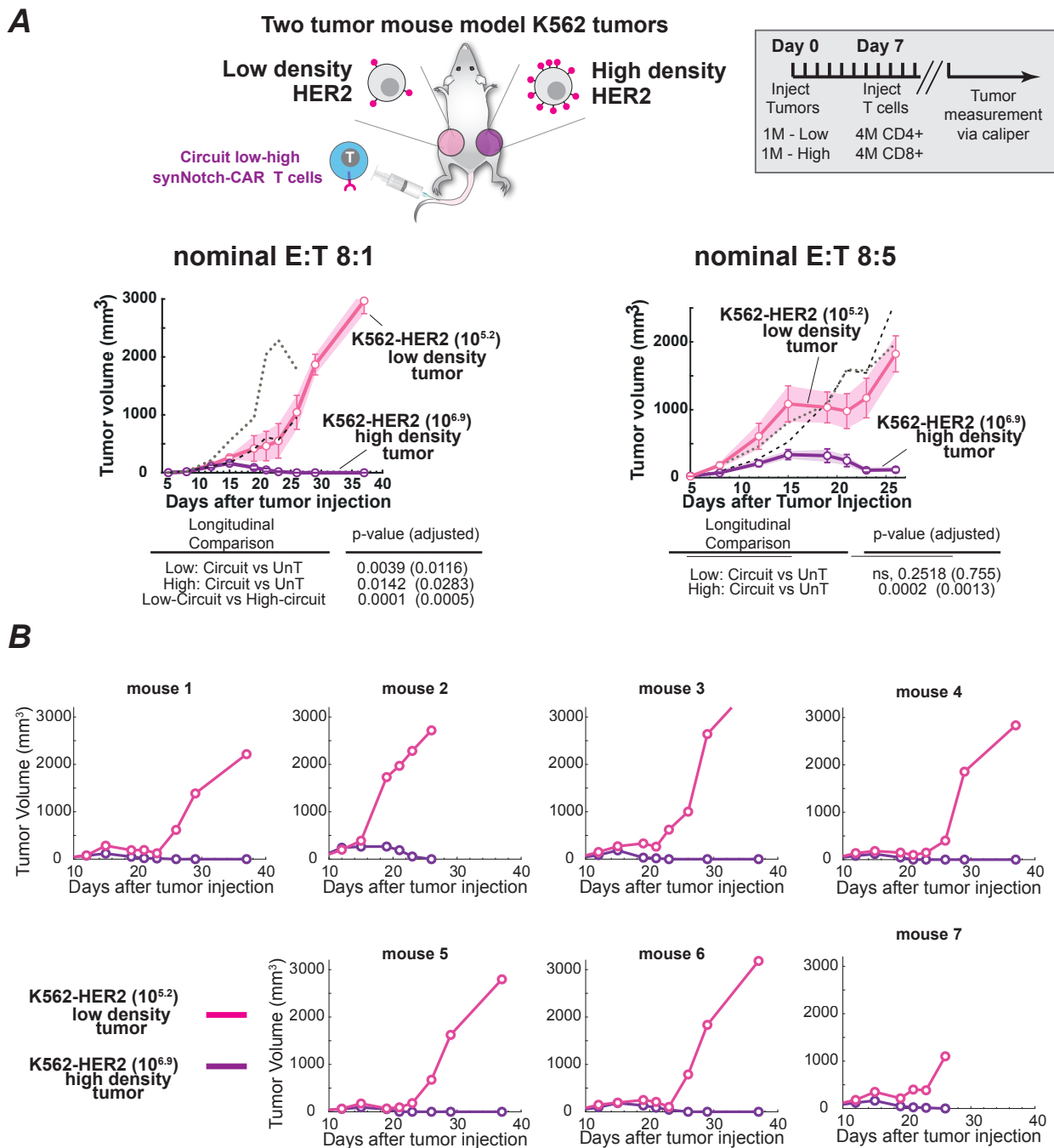


Figure S12. Low affinity synNotch to high affinity CAR circuit shows effective high vs low HER2 density tumor discrimination over at least 5-fold range of starting effector to target ratios (related to Fig. 4B).

A. Schematic of a two tumor mouse model experiment. Low- and high-expression engineered K562-HER2 tumor cells were injected subcutaneously in the flanks of N.S.G. mice at a dose of 1×10^6 cells per flank. Engineered primary human CD4+ and CD8+ T cells (4×10^6 cells of each type, 8×10^6 cells total dose) were injected i.v. 7 days after tumor injection. Tumor volume was monitored via caliper measurement over several days after tumor injection. The dark purple lines correspond to the high HER2 K562 tumor whereas the light pink lines correspond to the low HER2 K562 tumor ($n=7$). For comparison the curves for tumors implanted with 5×10^6 cells per flank are shown. **B.** Tumor volume data for individual mice treated with T cells expressing a low affinity synNotch to high affinity CAR circuit. The dark purple lines correspond to the high HER2 K562 tumor whereas the light pink lines correspond to the low HER2 K562 tumor.

Fig. S13. T cells expressing a two-step circuit low-to-high SynNotch-CAR affinity recognition circuit yield ultrasensitive antigen density sensing against EGFR engineered cells.

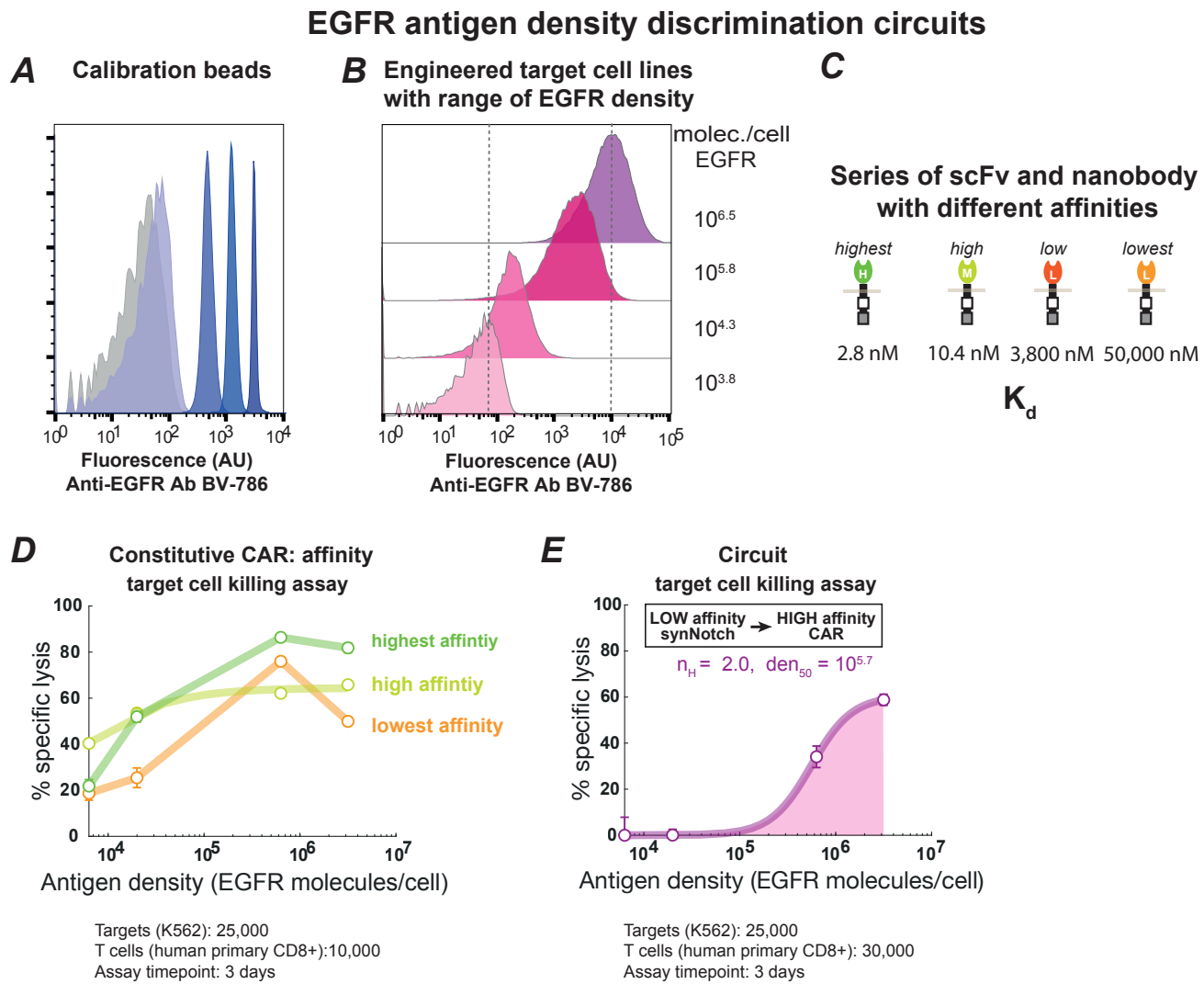


Figure S13. T cells expressing a two-step circuit low-to-high SynNotch-CAR affinity recognition circuit yield ultrasensitive antigen density sensing against EGFR engineered cells.

A. Representative flow cytometry histograms showing the fluorescence intensity of Quantum Simply Cellular anti-Mouse IgG beads (Bang Laboratories 815) stained with anti-EGFR BV786 antibody **B.** Representative flow cytometry histograms of engineered K562 EGFR cell lines stained with anti-EGFR BV786 antibody (n=3). The geometric mean of each population and the calibration curve built from data shown in the A was used to determine the average number of EGFR molecules per cell in each population. **C.** Series of scFv and nanobodies (30, 31) utilized to build two-step SynNotch to CAR circuits for EGFR density sensing. Their reported affinities are indicated. **D.** Target cell killing activity as a function of EGFR antigen density for T cells expressing CARs of indicated affinities. The E:T and assay time point are indicated. **E.** Target cell killing activity as a function of EGFR antigen density for T cells expressing a low affinity synNotch to high affinity CAR circuit. The percentage of specific lysis was determined using flow cytometry by counting the number of target cells after 3 days relative to a co-culture in the presence of untransduced T cells. Data are shown as the mean and standard error of the mean (n=3). For the circuit transparent line shows a fit to a hill equation, the hill coefficient and antigen density for half maximal activity are indicated (see Fig. S4A for equation details).

Movie S1. T cells expressing a high affinity CAR (shown in blue) co-cultured with either low HER2 density cancer cells (PC3 shown in green) or with high HER2 density cancer cells (SKOV3 shown in red), imaged for 3 days. Still images shown in Fig. 3B.

Movie S2. T cells expressing a low affinity synNotch to high affinity CAR circuit (shown in blue) co-cultured with either low HER2 density cancer cells (PC3 shown in green) or high HER2 density cancer cells (SKOV3 shown in red), imaged for 3 days. Still images shown in Fig. 3B.